JOURNAL OF GUIDANCE, CONTROL, AND DYNAMICS
Vol. 30, No. 4, July–August 2007

Nonlinear Synergetic Optimal Controllers

Nusawardhana,* S. H. Żak,† and W. A. Crossley‡
Purdue University, West Lafayette, Indiana 47907

DOI: 10.2514/1.27829

Optimality properties of synergetic controllers are analyzed using the Euler–Lagrange conditions and the Hamilton–Jacobi–Bellman equation. First, a synergetic control strategy is compared with the variable structure sliding mode control. The connections of synergetic control design methodology and the methods of variable structure sliding mode control are established. In fact, the methods of sliding surface design for the sliding mode control are essential for designing invariant manifolds in the synergetic control approach. It is shown that the synergetic control strategy can be derived using tools from the calculus of variations. The synergetic control laws have a simple structure because they are derived from the associated first-order differential equation. It is also shown that the synergetic controller for a certain class of linear quadratic optimal control problems has the same structure as the one generated using the linear quadratic regulator approach by solving the associated Riccati equation. The synergetic optimal control and sliding mode control methodologies are applied to the nonlinear control of the wing-rock suppression problem. Two different wing-rock dynamic models are used to test the design of the synergetic and sliding mode controllers. The performance of the closed-loop systems driven by these controllers is analyzed and compared.

Nomenclature

$\boldsymbol{A}$	=	state matrix in $\mathbb{R}^{n\times n}$
$\boldsymbol{A}(\boldsymbol{x})$	=	state-dependent vector function of dimension n
$\boldsymbol{A}_r$	=	state matrix of reduced-order design model
$\boldsymbol{B}$	=	input matrix in $\mathbb{R}^{n\times m}$
$\boldsymbol{B}(\boldsymbol{x})$	=	state-dependent input matrix function of size $n \times m$
$\boldsymbol{B}_r$	=	input matrix of reduced-order design model
$\boldsymbol{I}_m$	=	identity matrix in $\mathbb{R}^{m\times m}$
J	=	numerical value of the cost functional in optimal control problems
K	=	gain of discontinuous control in sliding mode controller
$L(\cdot)$	=	cost functional integrand
$\mathcal{M}$	=	manifold $\{\boldsymbol{x}\colon \boldsymbol{\sigma}(\boldsymbol{x}) = \boldsymbol{0}\}$ of dimension $n - m$
$\boldsymbol{N}$	=	weight matrix for cross term between state and control variables in LQR integrand
$\boldsymbol{O}$	=	zero matrix
$\boldsymbol{P}$, $\tilde{\boldsymbol{P}}$	=	matrices, solutions to Riccati equation, or algebraic HJB equation
$\boldsymbol{Q}$	=	weight matrix for state variables in LQR integrand
$\boldsymbol{R}$	=	weight matrix for control variables in LQR integrand
$\boldsymbol{S}$	=	surface/hyperplane matrix
$\boldsymbol{S}_r$	=	surface/hyperplane matrix in reduced-order control design
s	=	Laplace variable, or differentiation operator
$\boldsymbol{s}(\boldsymbol{x})$	=	state-dependent surface function
T	=	positive design parameter
$\boldsymbol{T} = \boldsymbol{T}^\top > 0$	=	symmetric positive definite constant matrix, design parameter matrix
$\boldsymbol{u}$	=	input vector of dimension m
$\boldsymbol{u}_d$	=	discontinuous control component
$\boldsymbol{u}_s$	=	continuous control component
$\boldsymbol{u}_{\text{eq}}$	=	equivalent control
V	=	value function in optimal control problem
$\boldsymbol{W}^g$	=	matrix orthogonal to $\boldsymbol{B}$, generalized inverse to $\boldsymbol{W}$, so that $\boldsymbol{W}\boldsymbol{W}^g = \boldsymbol{I}_{n-m}$
$\boldsymbol{x}$	=	state variable vector of dimension n
$\boldsymbol{x}_r$	=	state variable vector of reduced-order dynamic model
α_i	=	ith parameter of wing-rock dynamic model
β	=	parameter related to actuator input in wing-rock dynamic model
δ_a	=	actuator state variable in wing-rock dynamic model
λ	=	adjustable parameter used in the design of $\boldsymbol{S}$
σ, $\sigma(\mathbf{x})$	=	aggregated variable of $\boldsymbol{x}$ defining the manifold $\mathcal{M}$
ϕ	=	roll angle
$\dot{\phi}$	=	roll rate
$\boldsymbol{\Psi}$, $\boldsymbol{\Phi}$	=	variables appearing in algebraic matrix Riccati equation

I. Introduction

THE objective of the optimal control problem (see, for example, [1], Chap. 5) is to find an admissible control strategy that ensures the completion of control objective and leads to optimization of a given performance index. In most cases, solving the nonlinear dynamical systems optimal control problem is not straightforward. Based upon sufficient optimality conditions, solving the associated nonlinear partial differential equation, known as the Hamilton–Jacobi–Bellman (HJB) equation [2–6], provides the solution to such problems. A closed-form solution is often difficult to obtain especially for nonlinear dynamical systems. However for a class of nonlinear dynamical systems with a special cost functional, solving a first-order differential equation produces a closed-form analytical solution to a class of optimal control problems. This first-order differential equation plays an essential role in the synergetic control methodology.

Kolesnikov and coworkers [7] developed the method of synergetic control, and they, and others, later applied synergetic control to a number of industrial processes, including problems in power

Received 15 September 2006; revision received 4 December 2006; accepted for publication 14 January 2007.

*Graduate Student, School of Aeronautics and Astronautics, 315 North Grant Street. Student Member AIAA.

†Professor, School of Electrical and Computer Engineering, Electrical Engineering Building, 465 Northwestern Avenue.

‡Associate Professor, School of Aeronautics and Astronautics, 315 North Grant Street. Associate Fellow AIAA.

generation [8–12]. The synergetic control approach was also applied to adaptive control of nonlinear systems using neural networks [13]. The resulting synergetic control structure is attractive, because it is derived from a first-order differential equation related to optimality criteria. The authors of the above publications, however, do not elaborate on the derivation of synergetic control. Some state that synergetic control can be derived from functional optimization, but they do not state whether necessary or sufficiency conditions lead to the control structure.

The first objective of this paper is to present our derivation of the synergetic controller and to establish the connections with the variable structure sliding mode control approach. We show that the synergetic control for linear systems is a linear approximation of the nonlinear variable structure sliding mode controller. The linearity of the synergetic controller for linear systems is used to prove the stability of the closed-loop system driven by the synergetic controller. The second objective is to show that synergetic control not only satisfies the necessary condition for optimality but also satisfies the sufficient condition for optimality. The third objective is to show that, for linear time-invariant (LTI) systems and for a special form of the performance index, the synergetic control approach yields the same controller structure as the linear quadratic regulator approach. This is an especially attractive feature of synergetic controllers for a class of LTI optimal control problems, because the synergetic controllers result from solving a first-order differential equation while the linear quadratic regulator (LQR) design relies on solving the quadratic Riccati equation. The fourth objective of the paper is to present a synergetic control design algorithm. The final objective is to apply the proposed method to the regulation of wing-rock problems and to compare the results using the proposed method with those using the variable structure control. Some results in this paper were reported by us in [14].

II. Controlling Nonlinear Systems

Consider the following model of a nonlinear dynamical system:

$$\dot{\boldsymbol{x}} = \boldsymbol{A}(\boldsymbol{x}) + \boldsymbol{B}(\boldsymbol{x})\boldsymbol{u} \tag{1}$$

where $\boldsymbol{x} \in \mathbb{R}^n$ and $\boldsymbol{u} \in \mathbb{R}^m$. Thus, $\boldsymbol{A}(\boldsymbol{x}) \in \mathbb{R}^n$ and $\boldsymbol{B}(\boldsymbol{x}) \in \mathbb{R}^{n\times m}$. We discuss now a general method for stabilization and control of such systems. We refer to this approach as the stabilization and control via system restriction and manifold invariance. It consists of two steps:

1) Construction of a manifold

$$\mathcal{M} = \{\boldsymbol{x}\colon \boldsymbol{\sigma} = \boldsymbol{s}(\boldsymbol{x}) = \boldsymbol{0}, \boldsymbol{s}(\boldsymbol{x}) \in \mathbb{R}^m\}$$

so that

$$\det\left(\frac{\partial \boldsymbol{\sigma}}{\partial \boldsymbol{x}}\boldsymbol{B}(\boldsymbol{x})\right) \neq 0$$

and the system restricted to $\mathcal{M}$ behaves in a prespecified manner. For example, the trajectories of the system restricted to $\mathcal{M}$ asymptotically converge to a predetermined point $\boldsymbol{x}^* \in \mathcal{M}$. In the above, we used the following convention:

$$\frac{\partial \boldsymbol{\sigma}}{\partial \boldsymbol{x}} = \left(\frac{\partial}{\partial \boldsymbol{x}}\boldsymbol{s}(\boldsymbol{x})\right)^\top \in \mathbb{R}^{m\times n}$$

2) Construction of a controller that steers the system trajectories to the manifold $\mathcal{M}$ and then forces the trajectories to stay on the manifold thereafter.

A simple condition guaranteeing that the system trajectories are directed toward the manifold $\mathcal{M}$ is

$$\frac{\mathrm{d}}{\mathrm{d}t}\|\boldsymbol{\sigma}\|^2 = 2\boldsymbol{\sigma}^\top\dot{\boldsymbol{\sigma}} < 0 \quad \text{for } \boldsymbol{\sigma} \neq \boldsymbol{0} \tag{2}$$

The variable structure sliding mode control design is an example of this two-step approach to stabilizing nonlinear systems. We briefly elaborate on this approach. We observe that a trajectory is confined to the manifold $\mathcal{M}$ if and only if $\boldsymbol{\sigma}(\boldsymbol{x}) = \boldsymbol{0}$ and $\dot{\boldsymbol{\sigma}}(\boldsymbol{x}) = \boldsymbol{0}$. Solving $\dot{\boldsymbol{\sigma}}(\boldsymbol{x}) = \boldsymbol{0}$ for $\boldsymbol{u}$ yields a controller that forces a trajectory to lie on a level surface of $\boldsymbol{\sigma}(\boldsymbol{x})$. This controller is referred to, in the literature, as the equivalent controller and is denoted $\boldsymbol{u}_{\mathrm{eq}}$. To proceed, let

$$\frac{\partial \boldsymbol{\sigma}}{\partial \boldsymbol{x}} = \left(\frac{\partial}{\partial \boldsymbol{x}}\boldsymbol{s}(\boldsymbol{x})\right)^\top = \boldsymbol{s}_x(\boldsymbol{x}) \in \mathbb{R}^{m\times n}$$

Then, we have

$$\dot{\boldsymbol{\sigma}}(\boldsymbol{x}) = \boldsymbol{s}(\boldsymbol{x})\dot{\boldsymbol{x}} = \boldsymbol{s}_x(\boldsymbol{x})\boldsymbol{A}(\boldsymbol{x}) + \boldsymbol{s}_x(\boldsymbol{x})\boldsymbol{B}(\boldsymbol{x})\boldsymbol{u}_{\mathrm{eq}} = \boldsymbol{0}$$

Hence,

$$\boldsymbol{u}_{\mathrm{eq}} = -(\boldsymbol{s}_x(\boldsymbol{x})\boldsymbol{B}(\boldsymbol{x}))^{-1}\boldsymbol{s}_x(\boldsymbol{x})\boldsymbol{A}(\boldsymbol{x}) \tag{3}$$

Thus, the system dynamics restricted to the manifold $\mathcal{M} = \{\boldsymbol{x}\colon \boldsymbol{\sigma} = \boldsymbol{s}(\boldsymbol{x}) = \boldsymbol{0}\}$ are described by the equations

$$\boldsymbol{\sigma} = \boldsymbol{0} \tag{4}$$

$$\dot{\boldsymbol{x}} = \boldsymbol{A}(\boldsymbol{x}) + \boldsymbol{B}(\boldsymbol{x})\boldsymbol{u}_{\mathrm{eq}} = (\boldsymbol{I}_n - \boldsymbol{B}(x)(\boldsymbol{s}_x(\boldsymbol{x})\boldsymbol{B}(\boldsymbol{x}))^{-1}\boldsymbol{s}_x(\boldsymbol{x}))\boldsymbol{A}(\boldsymbol{x}) \tag{5}$$

Combining Eqs. (4) and (5) gives a reduced-order, $(n-m)$-dimensional dynamical system. This order reduction can be effectively exploited in the construction of the manifold $\{\boldsymbol{x}\colon \boldsymbol{\sigma} = \boldsymbol{0}\}$ resulting in a prespecified behavior of the system restricted to the manifold. Once the manifold is constructed, the next step is the controller design. Among many possible controller architectures that satisfy condition (2), the following variable structure sliding mode controller was analyzed in depth in [15],

$$\boldsymbol{u} = \boldsymbol{u}_{\mathrm{eq}} + \boldsymbol{u}_d \tag{6}$$

where

$$\boldsymbol{u}_d = -\eta(\boldsymbol{s}_x(\boldsymbol{x})\boldsymbol{B}(\boldsymbol{x}))^{-1}\frac{\boldsymbol{\sigma}(\boldsymbol{x})}{\|\boldsymbol{\sigma}(\boldsymbol{x})\|} \tag{7}$$

is the discontinuous component of $\boldsymbol{u}$. The controller gain $\eta > 0$ is a design parameter.

It is easy to show that the control law given by Eq. (6) satisfies condition (2). Indeed,

$$\frac{\mathrm{d}}{\mathrm{d}t}\|\boldsymbol{\sigma}\|^2 = 2\boldsymbol{\sigma}^\top\dot{\boldsymbol{\sigma}} = 2\boldsymbol{\sigma}^\top\boldsymbol{s}_x(\boldsymbol{x})\dot{\boldsymbol{x}} = 2\boldsymbol{\sigma}^\top(\boldsymbol{s}_x(\boldsymbol{x})\boldsymbol{A}(\boldsymbol{x}) + \boldsymbol{s}_x(\boldsymbol{x})\boldsymbol{B}(\boldsymbol{x})\boldsymbol{u})$$

$$= 2\boldsymbol{\sigma}^\top\left(\boldsymbol{s}_x(\boldsymbol{x})\boldsymbol{A}(\boldsymbol{x}) - (\boldsymbol{s}_x(\boldsymbol{x})\boldsymbol{B}(\boldsymbol{x}))\left((\boldsymbol{s}_x(\boldsymbol{x})\boldsymbol{B}(\boldsymbol{x}))^{-1}\boldsymbol{s}_x(\boldsymbol{x})\boldsymbol{A}(\boldsymbol{x})\right.\right.$$

$$\left.\left. + \eta(\boldsymbol{s}_x(\boldsymbol{x})\boldsymbol{B}(\boldsymbol{x}))^{-1}\frac{\boldsymbol{\sigma}}{\|\boldsymbol{\sigma}\|}\right)\right) = -2\eta\frac{\|\boldsymbol{\sigma}\|^2}{\|\boldsymbol{\sigma}\|} = -2\eta\|\boldsymbol{\sigma}\| < 0$$

for $\boldsymbol{\sigma} \neq \boldsymbol{0}$

Suppose now that we wish to construct a controller that would force the trajectories to approach the manifold $\mathcal{M} = \{\boldsymbol{\sigma} = \boldsymbol{0}\}$ exponentially as described by

$$\boldsymbol{T}\dot{\boldsymbol{\sigma}} + \boldsymbol{\sigma} = \boldsymbol{0} \tag{8}$$

where $\boldsymbol{T} = \boldsymbol{T}^\top > 0$ is a symmetric positive definite matrix, a design parameter matrix. It follows from Eq. (8) that

$$\dot{\boldsymbol{\sigma}} = -\boldsymbol{T}^{-1}\boldsymbol{\sigma} \tag{9}$$

Note that if we construct a controller that satisfies Eq. (8), then using Eq. (9), we obtain

$$\frac{\mathrm{d}}{\mathrm{d}t}\|\boldsymbol{\sigma}\|^2 = 2\boldsymbol{\sigma}^\top\dot{\boldsymbol{\sigma}} = -2\boldsymbol{\sigma}^\top\boldsymbol{T}\dot{\boldsymbol{\sigma}} < 0 \quad \text{for } \boldsymbol{\sigma} \neq \boldsymbol{0}$$

Thus, the "design condition" (2) is satisfied for such a control law. We now derive a control that satisfies the condition (8). Because $\boldsymbol{\sigma} = \boldsymbol{s}(\boldsymbol{x})$, $\dot{\boldsymbol{\sigma}} = \boldsymbol{s}_x(\boldsymbol{x})\dot{\boldsymbol{x}}$, hence Eq. (8) can be represented as

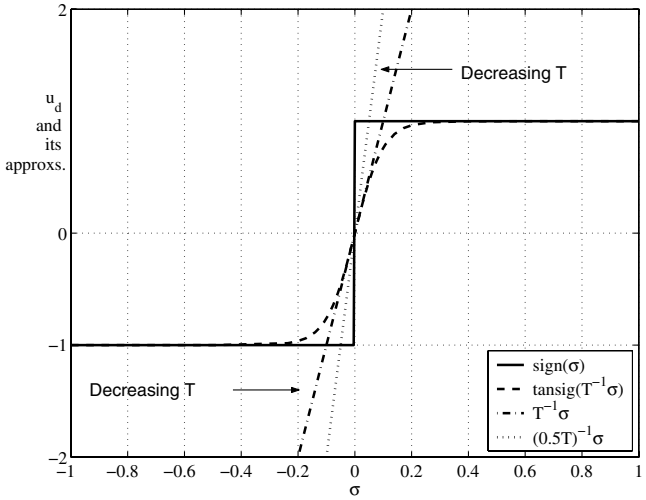

Fig. 1 The synergetic controller component u_s as a linear approximation to u_d for the scalar case when $s_x(x)B(x) = 1$ and $\eta = 1$.

$$\begin{aligned} T\dot{\sigma} + \sigma &= Ts_x(x)\dot{x} + s(x) = Ts_x(x)(A(x) + B(x)u) + s(x) \\ &= Ts_x(x)B(x)u + Ts_x(x)A(x) + s(x) = 0 \end{aligned}$$

The resulting control law obtained from the last equality takes the form,

$$\begin{aligned} u &= -(Ts_x(x)B(x))^{-1}(Ts_x(x)A(x) + s(x)) \\ &= -(s_x(x)B(x))^{-1}s_x(x)A(x) - (s_x(x)B(x))^{-1}T^{-1}s(x) \\ &= u_{\text{eq}} + u_s \end{aligned} \tag{10}$$

where

$$u_s = -(s_x(x)B(x))^{-1}T^{-1}s(x) \tag{11}$$

In Eq. (11), u_s denotes a smooth component of the resulting control law. The control law given by Eq. (10) is referred to as the nonlinear synergetic controller. This controller forces the system trajectories to approach the manifold asymptotically. When the trajectory starts on the manifold, the synergetic controller will maintain it there thereafter. The advantage of the synergetic controller over the control law given by Eq. (6) is that the synergetic controller is smooth while the sliding mode controller is discontinuous. However, the control law (6) forces the system trajectory onto the manifold in a finite time, and it maintains the trajectory on the manifold thereafter.

When we compare u_d, appearing in Eq. (7), and u_s from Eq. (11), we can conclude that u_s is a linear approximation to u_d. We consider a linear case when both u_d and u_s are scalar. In this case, $s_x(x)B(x)$ is a scalar. Plots in Fig. 1 indicate that as T decreases, the gain $1/T$ increases and u_s closely approximates u_d in its discontinuous region. We also show in Fig. 1 a plot of a smooth continuous tangential-sigmoid function approximating u_d. Using the tangential-sigmoid function to approximate u_d, or any other boundary-layer type approximation [16], yields a nonlinear controller, even though the approximation results in a smooth control law. The use of the linear approximation of u_d, on the other hand, allows us to use linear analysis techniques of closed-loop system stability properties.

In the following section, we consider a linear synergetic controller. For the linear case, we present a general algorithm for an invariant manifold construction and analyze the closed-loop system driven by the linear synergetic controller.

III. Linear Synergetic Control

We consider a linear time-invariant dynamical system model of the form,

$$\dot{x} = Ax + Bu \tag{12}$$

where $x = x(t) \in \mathbb{R}^n$, $u = u(t) \in \mathbb{R}^m$, and a linear manifold has the form

$$\sigma(x) = Sx = 0$$

where $S \in \mathbb{R}^{m\times n}$. Our goal is to construct a control strategy, $u = u(x)$, such that for any initial state x_0, the closed-loop system trajectory approaches the manifold $\sigma(x) = 0$ according to the policy $T\dot{\sigma} + \sigma = 0$. The relation $T\dot{\sigma} + \sigma = 0$ is central to the synergetic control approach. The rate with which the solutions of the above system of the first-order linear ordinary differential equation decay to zero can be controlled by appropriately selecting the matrix T. To proceed, note that

$$\dot{\sigma} = \left(\frac{\partial}{\partial x}\sigma(x)\right)^{\top}\dot{x} = S\dot{x}$$

Substituting the above into Eq. (8) yields

$$T\dot{\sigma} + \sigma = TS\dot{x} + Sx = TS(Ax + Bu) + Sx = 0$$

We assume that $\det(SB) \neq 0$. Hence,

$$u = -(TSB)^{-1}(TSA + S)x \tag{13}$$

The advantage of the above control strategy is that it is a linear controller that drives the system trajectory toward the manifold $\{Sx = 0\}$. Once on the manifold, or within a small neighborhood about the manifold, the system dynamics are of a reduced order. This order reduction can be exploited by the designer to shape the system dynamics when the system is moving along the manifold. A number of methods from the variable structure sliding mode control can be employed here to construct the matrix S of the linear invariant manifold; see, for example, Chap. 4 of [17], Secs. 3–4 in [18], Part II in [19], and pp. 333–336 in [20].

IV. Stability Analysis of a Linear Closed-Loop System Driven by Synergetic Controller

The synergetic control strategy (13) forces the system trajectory to asymptotically approach the manifold $\{\sigma = 0\}$. Thus, the closed-loop system will be asymptotically stable provided that the system (12) restricted to the manifold $\{\sigma = 0\}$ is asymptotically stable. In our proof of the above result, we use the following theorem from [20] on p. 333.

Theorem 1: Consider the system model, $\dot{x} = Ax + Bu$, where $\operatorname{rank}(B) = m$, the pair (A, B) is controllable, and a given set of $n - m$ complex numbers $\{\lambda_1, \ldots, \lambda_{n-m}\}$ is such that any λ_i whose imaginary part is nonzero appears in the above set in a conjugate pair. Then, there exist full-rank matrices $W \in \mathbb{R}^{n\times(n-m)}$ and $W^g \in \mathbb{R}^{(n-m)\times n}$ such that

$$W^g W = I_{n-m}, \qquad W^g B = O$$

and the eigenvalues of $W^g AW$ are

$$\operatorname{eig}(W^g AW) = \{\lambda_1, \ldots, \lambda_{n-m}\}$$

Furthermore, there exists a matrix $S \in \mathbb{R}^{m\times n}$ such that $SB = I_m$ and the system $\dot{x} = Ax + Bu$ restricted to $\{Sx = 0\}$ has its poles at $\lambda_1, \ldots, \lambda_{n-m}$. □

We can now state and prove the following theorem.

Theorem 2: If the manifold $\{Sx = 0\}$ is constructed so that the system $\dot{x} = Ax + Bu$ restricted to it is asymptotically stable and $\det(SB) \neq 0$, then the closed-loop system

$$\dot{x} = Ax + Bu, \qquad u = -(TSB)^{-1}(TSA + S)x$$

is asymptotically stable. □

Proof: Suppose that for a given set of complex numbers $\lambda_1, \ldots, \lambda_{n-m}$ whose real parts are negative, we constructed matrices $S \in \mathbb{R}^{m\times n}$, $W \in \mathbb{R}^{n\times(n-m)}$, and $W^g \in \mathbb{R}^{(n-m)\times n}$ that satisfy the conditions of Theorem 1. Note that we also have $SW = O$. We use

the following state-space transformation:

$$\boldsymbol{x} = [\boldsymbol{W} \quad \boldsymbol{B}]z$$

Note that the matrix $[\boldsymbol{W} \quad \boldsymbol{B}]$ is invertible and we can write

$$z = \begin{bmatrix} z_1 \\ z_2 \end{bmatrix} = [\boldsymbol{W} \quad \boldsymbol{B}]^{-1} = \begin{bmatrix} \boldsymbol{W}^g \\ \boldsymbol{S} \end{bmatrix}\boldsymbol{x}$$

In the new coordinates, the closed-loop system model takes the form,

$$\begin{bmatrix} \dot{z}_1 \\ \dot{z}_2 \end{bmatrix} = \begin{bmatrix} \boldsymbol{W}^g \\ \boldsymbol{S} \end{bmatrix}(\boldsymbol{A} - \boldsymbol{B}(\boldsymbol{SB})^{-1}\boldsymbol{T}^{-1}\boldsymbol{TSA} - \boldsymbol{B}(\boldsymbol{SB})^{-1}\boldsymbol{T}^{-1}\boldsymbol{S})[\boldsymbol{W} \quad \boldsymbol{B}]z = \begin{bmatrix} \boldsymbol{W}^g\boldsymbol{AW} & \boldsymbol{W}^g\boldsymbol{AB} \\ \boldsymbol{O} & -\boldsymbol{T}^{-1} \end{bmatrix}\begin{bmatrix} z_1 \\ z_2 \end{bmatrix} \tag{14}$$

Thus, the eigenvalues of the closed-loop system are the union of the eigenvalues of the matrices $\boldsymbol{W}^g\boldsymbol{AW}$ and $-\boldsymbol{T}^{-1}$. Because $\boldsymbol{T}$ is symmetric positive definite, the matrix $-\boldsymbol{T}^{-1}$ must have negative eigenvalues. By construction, the eigenvalues of $\boldsymbol{W}^g\boldsymbol{AW}$ are $\lambda_1, \ldots, \lambda_{n-m}$, which are located in the open left-half complex plane. Hence, the closed-loop system is asymptotically stable.

It follows from Eq. (14) that, when the closed-loop system motion is restricted to the manifold $\{z_2 = \boldsymbol{Sx} = \boldsymbol{0}\}$, and so $\dot{z}_2 = \boldsymbol{0}$, then its dynamics have the form

$$\dot{z}_1 = \boldsymbol{W}^g\boldsymbol{AW}z_1 \tag{15}$$

By construction, the eigenvalues of the above system are in the open left-half complex plane. □

Consider now the dynamical system described by

$$\left.\begin{aligned} \dot{\boldsymbol{x}} &= \boldsymbol{Ax} + \boldsymbol{Bu} \\ \boldsymbol{\sigma} &= \boldsymbol{Sx} \end{aligned}\right\} \tag{16}$$

where $\boldsymbol{S} \in \mathbb{R}^{m\times n}$ and $\boldsymbol{SB}$ is invertible. The system zeros of the above dynamical system are the zeros of the determinant of the system matrix

$$\begin{bmatrix} s\boldsymbol{I}_n - \boldsymbol{A} & \boldsymbol{B} \\ \boldsymbol{S} & \boldsymbol{O} \end{bmatrix}$$

It is shown in [20] on p. 329 that the system zeros of Eq. (16) are the poles of the reduced-order system given by Eq. (15) above, which are the poles of the system modeled by

$$\left.\begin{aligned} \dot{\boldsymbol{x}} &= (\boldsymbol{I}_n - \boldsymbol{B}(\boldsymbol{SB})^{-1}\boldsymbol{S})\boldsymbol{Ax} \\ \boldsymbol{Sx} &= \boldsymbol{0} \end{aligned}\right\} \tag{17}$$

Thus, the invariant manifold design can be viewed as constructing an output matrix $\boldsymbol{S}$ so that the system (16) has a set of its system zeros in desired locations.

V. Synergetic Control Development Using the Euler–Lagrange Equation

We now use a calculus of variations to analyze synergetic controllers. The simplest variational problem [21,22] can be formulated as follows.

Let $L(t, \boldsymbol{x}, \dot{\boldsymbol{x}})$ be a function with continuous first and second derivatives with respect to all of its arguments. Among all of the feasible $\boldsymbol{x}(t)$ that are continuously differentiable for $t_0 \le t \le t_f$ and satisfy boundary conditions

$$\boldsymbol{x}(t_0) = \boldsymbol{x}_0, \qquad \boldsymbol{x}(t_f) = \boldsymbol{x}_f$$

find the function $\boldsymbol{x}(t)$ for which the functional

$$J = \int_{t_0}^{t_f} L(t, \boldsymbol{x}, \dot{\boldsymbol{x}})\,\mathrm{d}t \tag{18}$$

has an extremum.

A necessary condition for the functional J in Eq. (18) to have an extremum is given by the following theorem.

Theorem 3 (A Necessary Extremum Condition [21]): Let

$$J = \int_{t_0}^{t_f} L(t, \boldsymbol{x}, \dot{\boldsymbol{x}})\,\mathrm{d}t$$

be a functional defined on the set of functions $\boldsymbol{x}(t)$ that have continuous first derivatives in $[t_0, t_f]$ and satisfy boundary conditions $\boldsymbol{x}(t_0) = \boldsymbol{x}_0$ and $\boldsymbol{x}(t_f) = \boldsymbol{x}_f$. Then a necessary condition for $\boldsymbol{x}(t)$ to be an extremizer of $J(\boldsymbol{x}(t_0))$ is that $\boldsymbol{x}(t)$ satisfies the Euler–Lagrange equation

$$\frac{\mathrm{d}}{\mathrm{d}t}\left(\frac{\partial L}{\partial \dot{\boldsymbol{x}}}\right) - \frac{\partial L}{\partial \boldsymbol{x}} = \boldsymbol{0} \tag{19}$$

□

In other words, if $\boldsymbol{x}^*(t)$ is a local minimizer of J on all admissible functions $\boldsymbol{x}(t)$ in the interval $t_0 \le t \le t_f$, then $\boldsymbol{x}^*(t)$ satisfies

$$\frac{\mathrm{d}}{\mathrm{d}t}\left(\frac{\partial}{\partial \dot{\boldsymbol{x}}}L(t, \boldsymbol{x}^*, \dot{\boldsymbol{x}}^*)\right) - \frac{\partial}{\partial \boldsymbol{x}}L(t, \boldsymbol{x}^*, \dot{\boldsymbol{x}}^*) = \boldsymbol{0}$$

To proceed, let

$$L(t, \boldsymbol{\sigma}, \dot{\boldsymbol{\sigma}}) = \dot{\boldsymbol{\sigma}}^\top\boldsymbol{T}^\top\boldsymbol{T}\dot{\boldsymbol{\sigma}} + \boldsymbol{\sigma}^\top\boldsymbol{\sigma} \tag{20}$$

where $\boldsymbol{\sigma}(t) \in \mathbb{R}^m$, $\dot{\boldsymbol{\sigma}}(t) \in \mathbb{R}^m$ is the first-order time derivative of $\boldsymbol{\sigma}(t)$, and $\boldsymbol{T} = \boldsymbol{T}^\top > 0$ is a symmetric positive definite matrix. For notational simplicity, the argument t in $\boldsymbol{\sigma}$ and $\dot{\boldsymbol{\sigma}}$ will be omitted. We wish to find a minimum of the functional

$$J = \int_{t_0}^{\infty} L(t, \boldsymbol{\sigma}, \dot{\boldsymbol{\sigma}})\,\mathrm{d}t = \int_{t_0}^{\infty} (\dot{\boldsymbol{\sigma}}^\top\boldsymbol{T}^\top\boldsymbol{T}\dot{\boldsymbol{\sigma}} + \boldsymbol{\sigma}^\top\boldsymbol{\sigma})\,\mathrm{d}t \tag{21}$$

By Theorem 3, if $\boldsymbol{\sigma}$ is to be an extremizer of $J(\boldsymbol{\sigma})$ given by Eq. (21), then it must satisfy the Euler–Lagrange equation given by Eq. (19). Substituting $L(t, \boldsymbol{\sigma}, \dot{\boldsymbol{\sigma}})$ given by Eq. (20) into (19) and using the fact that the symmetric positive definite $\boldsymbol{T} = \boldsymbol{T}^\top$, we obtain

$$\begin{aligned} &\frac{\mathrm{d}}{\mathrm{d}t}\left(\frac{\partial L(t, \boldsymbol{\sigma}, \dot{\boldsymbol{\sigma}})}{\partial \dot{\boldsymbol{\sigma}}}\right) - \frac{\partial L(t, \boldsymbol{\sigma}, \dot{\boldsymbol{\sigma}})}{\partial \boldsymbol{\sigma}} = \frac{\mathrm{d}}{\mathrm{d}t}\left(\frac{\partial}{\partial \dot{\boldsymbol{\sigma}}}\{\dot{\boldsymbol{\sigma}}^\top\boldsymbol{T}^\top\boldsymbol{T}\dot{\boldsymbol{\sigma}} + \boldsymbol{\sigma}^\top\boldsymbol{\sigma}\}\right) \\ &- \frac{\partial}{\partial \boldsymbol{\sigma}}\{\dot{\boldsymbol{\sigma}}^\top\boldsymbol{T}^\top\boldsymbol{T}\dot{\boldsymbol{\sigma}} + \boldsymbol{\sigma}^\top\boldsymbol{\sigma}\} = \frac{\mathrm{d}}{\mathrm{d}t}(2\boldsymbol{T}^\top\boldsymbol{T}\dot{\boldsymbol{\sigma}}) - 2\boldsymbol{\sigma} = 2\boldsymbol{T}^\top\boldsymbol{T}\frac{\mathrm{d}}{\mathrm{d}t}\left(\frac{\mathrm{d}}{\mathrm{d}t}\boldsymbol{\sigma}\right) \\ &- 2\boldsymbol{\sigma} = 2\boldsymbol{T}^2\left(\frac{\mathrm{d}}{\mathrm{d}t}\right)^2\boldsymbol{\sigma} - 2\boldsymbol{\sigma} = 2\left(\boldsymbol{T}\frac{\mathrm{d}}{\mathrm{d}t} + \boldsymbol{I}_m\right)^\top\left(\boldsymbol{T}\frac{\mathrm{d}}{\mathrm{d}t} - \boldsymbol{I}_m\right)\boldsymbol{\sigma} = \boldsymbol{0} \end{aligned} \tag{22}$$

A solution to Eq. (22) is given by one of the following equations:

$$\boldsymbol{T}\dot{\boldsymbol{\sigma}} + \boldsymbol{\sigma} = \boldsymbol{0} \quad \text{or} \quad \boldsymbol{T}\dot{\boldsymbol{\sigma}} - \boldsymbol{\sigma} = \boldsymbol{0}$$

We select the first equation, $\boldsymbol{T}\dot{\boldsymbol{\sigma}} + \boldsymbol{\sigma} = \boldsymbol{0}$, because it yields a stabilizing solution. We summarize the above development in the form of the following propositions:

Proposition 1: If $\boldsymbol{\sigma}^*$ is a local minimizer of the functional

$$J = \int_{t_0}^{\infty} (\dot{\boldsymbol{\sigma}}^\top\boldsymbol{T}^\top\boldsymbol{T}\dot{\boldsymbol{\sigma}} + \boldsymbol{\sigma}^\top\boldsymbol{\sigma})\,\mathrm{d}t \tag{23}$$

on all admissible vector functions of $\boldsymbol{\sigma}$, then

$$\boldsymbol{T}\dot{\boldsymbol{\sigma}}^* + \boldsymbol{\sigma}^* = \boldsymbol{0} \tag{24}$$

Such $\boldsymbol{\sigma}^*$ is called the extremizing $\boldsymbol{\sigma}$. □

As mentioned above, $\boldsymbol{T}\dot{\boldsymbol{\sigma}} + \boldsymbol{\sigma} = \boldsymbol{0}$ is a stabilizing solution, because Eq. (24) converges to $\boldsymbol{\sigma} = \boldsymbol{0}$ as $t \to \infty$.

Proposition 2: For a nonlinear dynamical system model,

$$\left.\begin{array}{c}\dot{\boldsymbol{x}} = \boldsymbol{A}(\boldsymbol{x}) + \boldsymbol{B}(\boldsymbol{x})\boldsymbol{u} \\ \boldsymbol{\sigma} = \boldsymbol{s}(\boldsymbol{x})\end{array}\right\} \tag{25}$$

where $\boldsymbol{s}_x(\boldsymbol{x})\boldsymbol{B}(\boldsymbol{x})$ is invertible, the control law

$$\boldsymbol{u}^* = -(\boldsymbol{T}\boldsymbol{s}_x(\boldsymbol{x})\boldsymbol{B}(\boldsymbol{x}))^{-1}(\boldsymbol{T}\boldsymbol{s}_x(\boldsymbol{x})\boldsymbol{A}(\boldsymbol{x}) + \boldsymbol{s}(\boldsymbol{x})) \tag{26}$$

derived from the first-order differential equation (24) is the extremizing controller for the optimal control problem with the performance index given by Eq. (23). □

It follows from the above that the extremizing control law for a linear time-invariant dynamical system modeled by Eq. (12) with the associated performance index (23) is given by Eq. (13).

VI. Background Results From Optimal Control

The cost functional used to derive the synergetic optimal control is related to the formulation of a linear quadratic optimal control problem with cross-product terms in the quadratic performance index. We briefly discuss this as an introduction for the following section's derivation of synergetic control based upon the sufficient optimality condition. Comprehensive discussion of optimal control with cross-product terms in the quadratic performance index can be found in [23] on pp. 56–57.

Consider a linear time-invariant dynamical system modeled by Eq. (12) and the associated performance index

$$J = \int_{t_0}^{\infty} (\boldsymbol{x}^\top \boldsymbol{Q}\boldsymbol{x} + 2\boldsymbol{x}^\top \boldsymbol{N}^\top \boldsymbol{u} + \boldsymbol{u}^\top \boldsymbol{R}\boldsymbol{u})\,\mathrm{d}t \tag{27}$$

where $\boldsymbol{Q} = \boldsymbol{Q}^\top \geq 0$, $\boldsymbol{N} \in \mathbb{R}^{m\times n}$, and $\boldsymbol{R} = \boldsymbol{R}^\top > 0$. The problem of determining an input $\boldsymbol{u}^* = \boldsymbol{u}^*(t)$, $t \geq t_0$, for the dynamical system (12) that minimizes the performance index (27) is called the deterministic linear quadratic optimal regulator problem. For the LQR problem, the control law

$$\boldsymbol{u}^* = -\boldsymbol{R}(\boldsymbol{B}^\top \tilde{\boldsymbol{P}} + \boldsymbol{N})\boldsymbol{x} \tag{28}$$

where the matrix $\tilde{\boldsymbol{P}}$ is the solution to

$$\boldsymbol{A}^\top \tilde{\boldsymbol{P}} + \tilde{\boldsymbol{P}}\boldsymbol{A} + \boldsymbol{Q} - (\boldsymbol{B}^\top \tilde{\boldsymbol{P}} + \boldsymbol{N})^\top \boldsymbol{R}^{-1}(\boldsymbol{B}^\top \tilde{\boldsymbol{P}} + \boldsymbol{N}) = \boldsymbol{O} \tag{29}$$

minimizes the performance index (27). The control law $\boldsymbol{u}^*$ given by Eq. (28), together with the solution $\tilde{\boldsymbol{P}}$ to Eq. (29), solves the associated HJB equation

$$\min_{\boldsymbol{u}}\left\{\frac{dV}{dt} + \boldsymbol{x}^\top \boldsymbol{Q}\boldsymbol{x} + 2\boldsymbol{x}^\top \boldsymbol{N}^\top \boldsymbol{u} + \boldsymbol{u}^\top \boldsymbol{R}\boldsymbol{u}\right\} = 0 \tag{30}$$

where $V = \min_{\boldsymbol{u}} J = \boldsymbol{x}^\top \tilde{\boldsymbol{P}}\boldsymbol{x}$.

VII. Sufficiency Condition for Optimality of Synergetic Controllers

Consider now a continuous-time nonlinear dynamical system modeled by

$$\dot{\boldsymbol{x}}(t) = \boldsymbol{f}(\boldsymbol{x}(t), \boldsymbol{u}(t)), \qquad t_0 \leq t \leq \infty, \qquad \boldsymbol{x}(t_0) = \boldsymbol{x}_0 \tag{31}$$

We wish to find a control strategy $\{\boldsymbol{u}(t)\colon t \in [t_0, \infty)\}$ that together with its corresponding state trajectory $\{\boldsymbol{x}_{\boldsymbol{u}}(t)\colon t \in [t_0, \infty)\}$ minimizes the performance index,

$$J = \int_{t_0}^{\infty} L(\boldsymbol{x}_{\boldsymbol{u}}(t), \boldsymbol{u}(t))\,\mathrm{d}t \tag{32}$$

This is an infinite-horizon optimal control problem. One way to synthesize an optimal feedback control $\boldsymbol{u}^*$ is to employ the following theorem that gives us a sufficiency condition for optimality of the resulting controller. This well-known theorem can be found, for example, in Vol. I, on p. 93 of [24].

Theorem 4: Suppose $V(\boldsymbol{x})$ is a solution to the HJB equation,

$$\min_{\boldsymbol{u}}\left\{\frac{dV(\boldsymbol{x})}{dt} + L(\boldsymbol{x}, \boldsymbol{u})\right\} = 0 \tag{33}$$

$$V(\boldsymbol{x}) \to 0 \quad \text{as} \quad t \to \infty \tag{34}$$

Suppose that $\boldsymbol{u}*$ is a minimizer of Eq. (33). Let $\boldsymbol{x}^*(t)$, $t \in [t_0, \infty)$ be the state trajectory emanating from the given initial condition $\boldsymbol{x}_0$ when the control $\boldsymbol{u}^*(t)$ is applied, that is, $\boldsymbol{x}^*(t)$ satisfies $\dot{\boldsymbol{x}}^*(t) = \boldsymbol{f}(\boldsymbol{x}^*(t), \boldsymbol{u}^*(t))$ subject to the initial condition $\boldsymbol{x}^*(t_0) = \boldsymbol{x}_0$. Then V is the unique solution to the HJB equation, that is,

$$V(\boldsymbol{x}) = \min_{\boldsymbol{u}} J(\boldsymbol{x}) = J^*(\boldsymbol{x})$$

□

Using the above condition, we now provide an optimal control structure for a class of nonlinear systems.

Proposition 3: Consider a nonlinear system model given by Eq. (25), where $\boldsymbol{s}_x(\boldsymbol{x})\boldsymbol{B}(\boldsymbol{x})$ is invertible, and the associated performance index,

$$J = \int_{t_0}^{\infty} L(\boldsymbol{\sigma}(t), \dot{\boldsymbol{\sigma}}(t))\,\mathrm{d}t \tag{35}$$

where

$$L(\boldsymbol{\sigma}, \dot{\boldsymbol{\sigma}}) = \dot{\boldsymbol{\sigma}}^\top \boldsymbol{T}^\top \boldsymbol{T}\dot{\boldsymbol{\sigma}} + \boldsymbol{\sigma}^\top \boldsymbol{\sigma} \tag{36}$$

The feedback control law,

$$\begin{aligned}\boldsymbol{u}^* = &-((\boldsymbol{s}_x(\boldsymbol{x})\boldsymbol{B}(\boldsymbol{x}))^\top \boldsymbol{T}^\top \boldsymbol{T}\boldsymbol{s}_x(\boldsymbol{x})\boldsymbol{B}(\boldsymbol{x}))^{-1}(\boldsymbol{s}_x(\boldsymbol{x})\boldsymbol{B}(\boldsymbol{x}))^\top \\ &\times (\boldsymbol{T}^\top \boldsymbol{T}\boldsymbol{s}_x(\boldsymbol{x})\boldsymbol{A}(\boldsymbol{x}) + \boldsymbol{T}\boldsymbol{s}(\boldsymbol{x}))\end{aligned}$$

minimizes the performance index (35). The above control law can be further simplified and represented in the form,

$$\boldsymbol{u}^* = -(\boldsymbol{T}\boldsymbol{s}_x(\boldsymbol{x})\boldsymbol{B}(\boldsymbol{x}))^{-1}(\boldsymbol{T}\boldsymbol{s}_x(\boldsymbol{x})\boldsymbol{A}(\boldsymbol{x}) + \boldsymbol{s}(\boldsymbol{x})) \tag{37}$$

The value of the performance index for this control problem is

$$V(\boldsymbol{\sigma}(t)) = J(\boldsymbol{\sigma}(t))|_{\boldsymbol{u}(t)=\boldsymbol{u}^*(t)} = \boldsymbol{\sigma}^\top(t)\boldsymbol{P}\boldsymbol{\sigma}(t) \tag{38}$$

where $\boldsymbol{P} = \boldsymbol{T} = \boldsymbol{T}^\top$. □

Proof: Our goal is to find a feedback controller that minimizes the performance index (35). Let

$$V(\boldsymbol{\sigma}(t)) = \min_{\boldsymbol{u}(t)} J(\boldsymbol{\sigma}(t)) = \boldsymbol{\sigma}^\top(t)\boldsymbol{P}\boldsymbol{\sigma}(t) \tag{39}$$

The HJB equation for the optimal control of dynamical system (25) with the associated performance index (35) is

$$\min_{\boldsymbol{u}(t)}\left\{\frac{\mathrm{d}}{\mathrm{d}t}V(\boldsymbol{\sigma}(t)) + L(\boldsymbol{\sigma}(t), \dot{\boldsymbol{\sigma}}(t))\right\} = 0 \tag{40}$$

To find the minimizing $\boldsymbol{u}$, we apply the first-order necessary condition for the unconstrained minimization to the expression within the curly bracket. Note that $\boldsymbol{\sigma}$ is not a function of $\boldsymbol{u}$. It is $\dot{\boldsymbol{\sigma}}$ that depends upon $\boldsymbol{u}$. We have

$$\begin{aligned}\frac{\partial}{\partial \boldsymbol{u}}&\left\{\frac{dV(\boldsymbol{\sigma}(t))}{dt} + L(\boldsymbol{\sigma}(t), \dot{\boldsymbol{\sigma}}(t))\right\} = \frac{\partial}{\partial \boldsymbol{u}}\left\{\frac{d\boldsymbol{\sigma}^\top \boldsymbol{P}\boldsymbol{\sigma}}{dt} + L(\boldsymbol{\sigma}, \dot{\boldsymbol{\sigma}})\right\} \\ &= \frac{\partial}{\partial \boldsymbol{u}}\{2\dot{\boldsymbol{\sigma}}^\top \boldsymbol{P}\boldsymbol{\sigma} + \dot{\boldsymbol{\sigma}}^\top \boldsymbol{T}^\top \boldsymbol{T}\dot{\boldsymbol{\sigma}} + \boldsymbol{\sigma}^\top \boldsymbol{\sigma}\} = \frac{\partial}{\partial \boldsymbol{u}}\{2(\boldsymbol{s}_x(\boldsymbol{x})\dot{\boldsymbol{x}})^\top \boldsymbol{P}\boldsymbol{\sigma} \\ &+ (\boldsymbol{s}_x(\boldsymbol{x})\dot{\boldsymbol{x}})^\top \boldsymbol{T}^\top \boldsymbol{T}\boldsymbol{s}_x(\boldsymbol{x})\dot{\boldsymbol{x}} + \boldsymbol{\sigma}^\top \boldsymbol{\sigma}\} = \frac{\partial}{\partial \boldsymbol{u}}\{2(\boldsymbol{s}_x(\boldsymbol{x})\boldsymbol{B}(\boldsymbol{x})\boldsymbol{u})^\top \boldsymbol{P}\boldsymbol{\sigma} \\ &+ 2(\boldsymbol{s}_x(\boldsymbol{x})\boldsymbol{B}(\boldsymbol{x})\boldsymbol{u})^\top \boldsymbol{T}^\top \boldsymbol{T}\boldsymbol{s}_x(\boldsymbol{x})\boldsymbol{A}(\boldsymbol{x}) \\ &+ (\boldsymbol{s}_x(\boldsymbol{x})\boldsymbol{B}(\boldsymbol{x})\boldsymbol{u})^\top \boldsymbol{T}^\top \boldsymbol{T}(\boldsymbol{s}_x(\boldsymbol{x})\boldsymbol{B}(\boldsymbol{x})\boldsymbol{u})\} = \boldsymbol{0}\end{aligned}$$

Observing that the last term in the above equation is quadratic in $\boldsymbol{u}$,

we obtain

$$(s_x(x)B(x))^\top P\sigma + (s_x(x)B(x))^\top T^\top T s_x(x)A(x) + (s_x(x)B(x))^\top T^\top T s_x(x)B(x)u = 0 \quad (41)$$

Solving the above for u gives

$$u^* = -((s_x(x)B(x))^\top T^\top T s_x(x)B(x))^{-1}(s_x(x)B(x))^\top (Ps(x) + T^\top T s_x(x)A(x))$$

Because $\sigma = s(x)$ is constructed in such a way that $s_x B(x)$ is invertible, the controller u^* above can further be simplified. Note also that T is symmetric and invertible. Hence,

$$u^* = -(Ts_x(x)B(x))^{-1}T^{-T}(s_x(x)B(x))^{-T}(s_x(x)B(x))^\top (Ps(x) + T^\top T s_x(x)A(x)) = -(Ts_x(x)B(x))^{-1}(T^{-T}Ps(x) + Ts_x(x)A(x)) \quad (42)$$

We substitute the control function u^* from Eq. (42) into the HJB equation (40) and solve the equation for P. In our manipulations we use the expression, $\dot\sigma = -T^{-1}\sigma$, to obtain

$$\frac{\mathrm{d}}{\mathrm{d}t}\sigma^\top P\sigma + L(\sigma,\dot\sigma) = \dot\sigma^\top P\sigma + \sigma^\top P\dot\sigma + \dot\sigma^\top T^\top T\dot\sigma + \sigma^\top\sigma = -(T^{-1}\sigma)^\top P\sigma - \sigma^\top PT^{-1}\sigma + \sigma^\top\sigma + \sigma^\top\sigma = -\sigma^\top T^{-T}P\sigma - \sigma^\top PT^{-1}\sigma + 2\sigma^\top\sigma = \sigma^\top(-T^{-T}P - PT^{-1} + 2I_m)\sigma = 0$$

from which we obtain

$$P = T = T^\top, \qquad P \in \mathbb{R}^{m\times m} \quad (43)$$

When we substitute P from Eq. (43) back into Eq. (42), we obtain the control law,

$$u^* = -(Ts_x(x)B(x))^{-1}(s(x) + Ts_x(x)A(x))$$

□

Note that if we premultiply Eq. (41) by $\{(s_x(x)B(x))^\top P\}^{-1}$ and use 1) $P = T = T^\top$ and 2) $\dot\sigma = s_x(x)(A(x) + B(x)u)$, we obtain the differential equation that plays a fundamental role in synergetic control,

$$T\dot\sigma + \sigma = 0$$

We use the above equation to construct the optimizing control laws (42) and ultimately Eq. (37).

The following theorem gives a sufficient condition for the LQR control strategy to take the form of the synergetic control law.

Theorem 5: Consider the LTI dynamic system modeled by

$$\left.\begin{aligned}\dot x &= Ax + Bu\\ \sigma &= Sx\end{aligned}\right\} \quad (44)$$

where S is constructed such that SB is invertible. Associated with the above LTI system (46) is the cost function

$$J = \int_{t_0}^{\infty}(\dot\sigma^\top T^\top T\dot\sigma + \sigma^\top\sigma)\,\mathrm{d}t = \int_{t_0}^{\infty}(\dot x^\top S^\top T^\top TS\dot x + x^\top S^\top Sx)\,\mathrm{d}t \quad (45)$$

The optimal controller has the form,

$$u^* = -(B^\top S^\top T^\top TSB)^{-1}(B^\top S^\top PS + B^\top S^\top T^\top TSA)x \quad (46)$$

where $P = T = T^\top \in \mathbb{R}^{m\times m}$. The control law (46) has the same form as the control law derived using the LQR approach to the system (44) together with the cost (45) reformulated as

$$J = \int_{t_0}^{\infty}(x^\top Qx + 2x^\top N^\top u + u^\top Ru)\,\mathrm{d}t \quad (47)$$

where

$$Q = A^\top S^\top T^\top TSA + S^\top S, \qquad N = B^\top S^\top T^\top TSA$$
$$R = B^\top S^\top T^\top TSB$$

Furthermore, since

$$\tilde P = S^\top PS$$

the control law (46) can be reformulated to the form of the synergetic control strategy,

$$u^* = -(TSB)^{-1}(TSA + S)x$$

□

Proof: We first construct the optimal feedback controller for Eq. (44) that minimizes Eq. (45). That is, we construct u so that

$$V(x(t_0)) = x^\top S^\top PSx = \min_u J(x(t_0))$$

The HJB equation for this LTI case has the form

$$\min_u\left\{\frac{\mathrm{d}}{\mathrm{d}t}x^\top S^\top PSx + \dot x^\top S^\top T^\top TS\dot x + x^\top S^\top Sx\right\} = 0 \quad (48)$$

from which we obtain the control law (46) using the same arguments as in the nonlinear case. This controller has a similar structure as the control law (42) in the nonlinear case analyzed above. Next, we substitute the control law (46) back into the HJB equation (48) to obtain

$$\dot x^\top S^\top PSx + x^\top S^\top PS\dot x + \dot x^\top S^\top T^\top TS\dot x + x^\top S^\top Sx = (Ax + Bu)^\top S^\top PSx + x^\top S^\top PS(Ax + Bu) + (Ax + Bu)^\top S^\top T^\top TS(Ax + Bu) + x^\top S^\top Sx = x^\top\Phi x = 0$$

where

$$\Phi = A^\top S^\top PS + S^\top PSA + A^\top S^\top T^\top TSA + S^\top S - \Psi^T(B^\top S^\top T^\top TSB)^{-1}\Psi \quad (49)$$

$$\Psi = B^\top S^\top PS + B^\top S^\top T^\top TSA \quad (50)$$

For the HJB equation to be satisfied, regardless of the value of x, the expression for Φ must be zero, which yields $P = T = T^\top \in \mathbb{R}^{m\times m}$. To see this, substitute $P = T = T^\top$ into the expression for Ψ given by Eq. (50) to obtain

$$\Psi = B^\top S^\top T^\top S + B^\top S^\top T^\top TSA = B^\top S^\top T^\top(TSA + S) \quad (51)$$

Substituting Ψ given by Eq. (51) into the last term of Eq. (49) yields

$$-\Psi^\top(B^\top S^\top T^\top TSB)^{-1}\Psi = -\Psi^\top(TSB)^{-1}(B^\top S^\top T^\top)^{-1}\Psi = -(S + TSA)^\top(TSA + S) = -S^\top S - A^\top S^\top T^\top S - S^\top TSA - A^\top S^\top T^\top TSA$$

which cancels out the first four terms in Eq. (49). These steps lead to the conclusion that $P = T$.

Note that because SB is invertible by construction, and $P = T = T^\top$ by Eq. (43), the control law (46) simplifies to

$$u^* = -(TSB)^{-1}(B^\top S^\top T^\top)^{-1}B^\top S^\top T^\top(S + TSA)x = -(TSB)^{-1}(TSA + S)x$$

which has the same form as the synergetic control law (13).

The solution to the LQR problem of the system (44) with the cost (47) is characterized by the matrix $\tilde P$ which is the solution to the Riccati equation

$$\begin{aligned}\boldsymbol{A}^{\top}\tilde{\boldsymbol{P}}+\tilde{\boldsymbol{P}}\boldsymbol{A}+\boldsymbol{Q}-(\boldsymbol{B}^{\top}\tilde{\boldsymbol{P}}+\boldsymbol{N})^{\top}\boldsymbol{R}^{-1}(\boldsymbol{B}^{\top}\tilde{\boldsymbol{P}}+\boldsymbol{N})&=\boldsymbol{A}^{\top}\tilde{\boldsymbol{P}}+\tilde{\boldsymbol{P}}\boldsymbol{A}\\&+\boldsymbol{A}^{\top}\boldsymbol{S}^{\top}\boldsymbol{T}^{\top}\boldsymbol{T}\boldsymbol{S}\boldsymbol{A}+\boldsymbol{S}^{\top}\boldsymbol{S}-(\boldsymbol{B}^{\top}\tilde{\boldsymbol{P}}\\&+\boldsymbol{B}^{\top}\boldsymbol{S}^{\top}\boldsymbol{T}^{\top}\boldsymbol{T}\boldsymbol{S}\boldsymbol{A})^{\top}(\boldsymbol{T}\boldsymbol{S}\boldsymbol{B})^{-1}(\boldsymbol{B}^{\top}\boldsymbol{S}^{\top}\boldsymbol{T}^{\top})^{-1}(\boldsymbol{B}^{\top}\tilde{\boldsymbol{P}}\\&+\boldsymbol{B}^{\top}\boldsymbol{S}^{\top}\boldsymbol{T}^{\top}\boldsymbol{T}\boldsymbol{S}\boldsymbol{A})=\boldsymbol{O}\end{aligned} \tag{52}$$

Using the matrix $\tilde{\boldsymbol{P}}$, the optimal feedback control of the associated LQR problem is

$$\begin{aligned}\boldsymbol{u}^{*}=-\boldsymbol{R}^{-1}(\boldsymbol{B}^{\top}\tilde{\boldsymbol{P}}+\boldsymbol{N})\boldsymbol{x}&=-(\boldsymbol{B}^{\top}\boldsymbol{S}^{\top}\boldsymbol{T}^{\top}\boldsymbol{T}\boldsymbol{S}\boldsymbol{B})^{-1}(\boldsymbol{B}^{\top}\tilde{\boldsymbol{P}}\\&+\boldsymbol{B}^{\top}\boldsymbol{S}^{\top}\boldsymbol{T}^{\top}\boldsymbol{T}\boldsymbol{S}\boldsymbol{A})\boldsymbol{x}\end{aligned} \tag{53}$$

Comparing Eqs. (49) and (52) together with Eq. (50), we see that $\tilde{\boldsymbol{P}}=\boldsymbol{S}^{\top}\boldsymbol{P}\boldsymbol{S}$. If we set $\tilde{\boldsymbol{P}}=\boldsymbol{S}^{\top}\boldsymbol{P}\boldsymbol{S}$ and take into account that $\boldsymbol{S}\boldsymbol{B}$ is invertible, then the above controller takes the form of the synergetic control law. □

It follows from the above that the control law derived from the first-order differential equation $\boldsymbol{T}\dot{\boldsymbol{\sigma}}+\boldsymbol{\sigma}=\boldsymbol{0}$ is not only extremizing, that is, this control law can be obtained from the Euler–Lagrange equation, but it is also optimizing in the sense that it can be obtained from the HJB equation.

It is well known that one can obtain the solution to the deterministic LQR problem from the HJB equation. Therefore, for the linear plant model and $\boldsymbol{\sigma}=\boldsymbol{S}\boldsymbol{x}$, we can obtain the optimizing control law,

$$\boldsymbol{u}^{*}=-(\boldsymbol{T}\boldsymbol{S}\boldsymbol{B})^{-1}(\boldsymbol{T}\boldsymbol{S}\boldsymbol{A}+\boldsymbol{S})\boldsymbol{x}$$

directly from the formula for the LQR control given by Eq. (28) in Sec. VI after making appropriate associations between the matrices of the performance indices,

$$J=\int_{t_0}^{\infty}(\boldsymbol{x}^{\top}\boldsymbol{Q}\boldsymbol{x}+2\boldsymbol{x}^{\top}\boldsymbol{N}^{\top}\boldsymbol{u}+\boldsymbol{u}^{\top}\boldsymbol{R}\boldsymbol{u})\,\mathrm{d}t$$

and

$$J=\int_{t_0}^{\infty}(\dot{\boldsymbol{\sigma}}^{\top}\boldsymbol{T}^{\top}\boldsymbol{T}\dot{\boldsymbol{\sigma}}+\boldsymbol{\sigma}^{\top}\boldsymbol{\sigma})dt=\int_{t_0}^{\infty}((\boldsymbol{S}\dot{\boldsymbol{x}})^{\top}\boldsymbol{T}^{\top}\boldsymbol{T}\boldsymbol{S}\dot{\boldsymbol{x}}+(\boldsymbol{S}\boldsymbol{x})^{\top}\boldsymbol{S}\boldsymbol{x})\,\mathrm{d}t$$

VIII. Synergetic Optimal Stabilizing Control

The problem of constructing an invariant manifold $\mathcal{M}=\{\boldsymbol{x}:\boldsymbol{\sigma}=\boldsymbol{0}\}$ such that the system confined to it is asymptotically stable has been addressed in the area of sliding mode control. The manifold construction in sliding mode control, for the LTI case, can be viewed as constructing the matrix $\boldsymbol{S}$ so that the system zeros (or zero dynamics for a general class of nonlinear systems) are asymptotically stable; see, for example, Sec. 6.5 in [20]. Therefore, various methods for constructing stable manifolds in sliding mode control are directly applicable for $\boldsymbol{\sigma}$ construction in the synergetic control; see, for example, Chap. 4 in [17], Secs. 3–4 in [18], Part II in [19], and pp. 333–336 in [20].

In the synergetic control approach, the controller $\boldsymbol{u}$ is designed by solving the first-order differential equation $\boldsymbol{T}\dot{\boldsymbol{\sigma}}+\boldsymbol{\sigma}=\boldsymbol{0}$, which induces the attractivity and invariance of the manifold $\boldsymbol{\sigma}=\boldsymbol{0}$.

We summarize this section with the following two-step design procedure:

1) Construct a stable hyperplane, or a manifold, $\mathcal{M}=\{\boldsymbol{x}:\boldsymbol{\sigma}=\boldsymbol{0}\}$.

2) Construct the optimizing control $\boldsymbol{u}$.

We illustrate the above considerations with a simple numerical example.

Example 1: Consider the double integrator state-space model,

$$\dot{\boldsymbol{x}}=\begin{bmatrix}0&1\\0&0\end{bmatrix}\boldsymbol{x}+\begin{bmatrix}0\\1\end{bmatrix}u \tag{54}$$

The control design objective for the system (54) is to regulate the state to the origin of $\mathbb{R}^2$ with a performance index to be determined. When σ is not properly constructed, the overall closed-loop system is unstable. The construction of σ, in this example, is concerned with selecting the row vector $\boldsymbol{s}$. Consider two candidates:

$$\boldsymbol{s}_{+}=[\,1\quad 1\,]\quad\text{and}\quad\boldsymbol{s}_{-}=[\,1\quad -1\,] \tag{55}$$

that yield $\sigma_{+}=\boldsymbol{s}_{+}\boldsymbol{x}$ and $\sigma_{-}=\boldsymbol{s}_{-}\boldsymbol{x}$, respectively. Associated with these matrices are the following performance indices:

$$J_{+}=\int_{t_0}^{\infty}\left(\dot{\sigma}_{+}^{2}+\sigma_{+}^{2}\right)\mathrm{d}t=\int_{t_0}^{\infty}\left(\boldsymbol{x}^{\top}\boldsymbol{Q}_{+}\boldsymbol{x}+2u\boldsymbol{N}_{+}\boldsymbol{x}+R_{+}u^{2}\right)\mathrm{d}t$$

and

$$J_{-}=\int_{t_0}^{\infty}\left(\dot{\sigma}_{-}^{2}+\sigma_{-}^{2}\right)\mathrm{d}t=\int_{t_0}^{\infty}(\boldsymbol{x}^{\top}\boldsymbol{Q}_{-}\boldsymbol{x}+2u\boldsymbol{N}_{-}\boldsymbol{x}+R_{-}u^{2})\,\mathrm{d}t$$

where

$$\begin{aligned}\boldsymbol{Q}_{+}&=\begin{bmatrix}1&+1\\+1&2\end{bmatrix},\qquad\boldsymbol{N}_{+}=[\,0\quad+1\,],\qquad R_{+}=[\,1\,]\\\boldsymbol{Q}_{-}&=\begin{bmatrix}1&-1\\-1&2\end{bmatrix},\qquad\boldsymbol{N}_{-}=[\,0\quad-1\,],\qquad R_{-}=[\,1\,]\end{aligned} \tag{56}$$

We selected $T=1$. We used MATLAB®, Version 6.5, to construct the LQR controllers. The results of the optimal control design using both the synergetic control and the LQR [Eq. (28)] for both cases $\boldsymbol{s}_{+}$ (denoted P_{+}) and $\boldsymbol{s}_{-}$ (denoted P_{-}) are summarized in Table 1. From this table, we can see that the LQR controllers for both cases yield stabilizing solutions. All closed-loop eigenvalues for both cases are negative. However, the synergetic controllers are critically dependent upon the selection of the manifold $\sigma=\boldsymbol{s}\boldsymbol{x}$. When $\boldsymbol{s}=\boldsymbol{s}_{+}$, the solution generated using the synergetic controller is the same as that obtained using the LQR method and results in negative closed-loop eigenvalues. However, when $\boldsymbol{s}=\boldsymbol{s}_{-}$, the closed-loop system driven by the synergetic controller has one positive closed-loop pole. The phase portraits of two closed-loop systems are shown in Fig. 2. The left plot corresponds to P_{+}, the right one corresponds to P_{-}. On both plots, solid lines indicate $\sigma_{+}=0$ and $\sigma_{-}=0$, while dashed lines indicate vectors perpendicular to both $\sigma_{+}=0$ and $\sigma_{-}=0$. Dashed arrows indicate the direction of trajectories approaching planes $\sigma_{+}=0$ and $\sigma_{-}=0$, while solid arrows indicate the direction of trajectories along manifolds $\sigma_{+}=0$ and $\sigma_{-}=0$.

In both cases, trajectories approach the respective manifolds, as expected. However, in the P_{+} case, state trajectories along the manifold $\sigma_{+}=0$ converge to the origin, while in the P_{-} case, state trajectories along the manifold $\sigma_{-}=0$ diverge from the origin. This is because motion along the manifold $\sigma_{-}=0$ is not stable, while the motion along the manifold $\sigma_{+}=0$ is stable.

Table 1 Comparison of the designs using the synergetic and LQR approaches

Problem	Controller, closed-loop poles	Synergetic	LQR
P_{+}	u^{*}	$-[\,1\quad 2\,]\boldsymbol{x}$	$-[\,1\quad 2\,]\boldsymbol{x}$
	$\lambda_{\text{c.l.}}$	$-1,-1$	$-1,-1$
P_{-}	u^{*}	$-[-1\quad 0\,]\boldsymbol{x}$	$-[\,1\quad 2\,]\boldsymbol{x}$
	$\lambda_{\text{c.l.}}$	$-1,+1$	$-1,-1$

IX. Synergetic Control Design for Wing-Rock Suppression

The wing-rock phenomenon manifests itself in the form of a sustained limit-cycle oscillation that limits the potential maneuver performance of an aircraft. There are diverse nonlinear models representing the wing-rock phenomenon [25–28]. For the purpose of control design, we employ two dynamical models: 1) second-order model [29], and 2) third-order model [30,31]. The main distinction between the two models lies in the modeling of the actuator

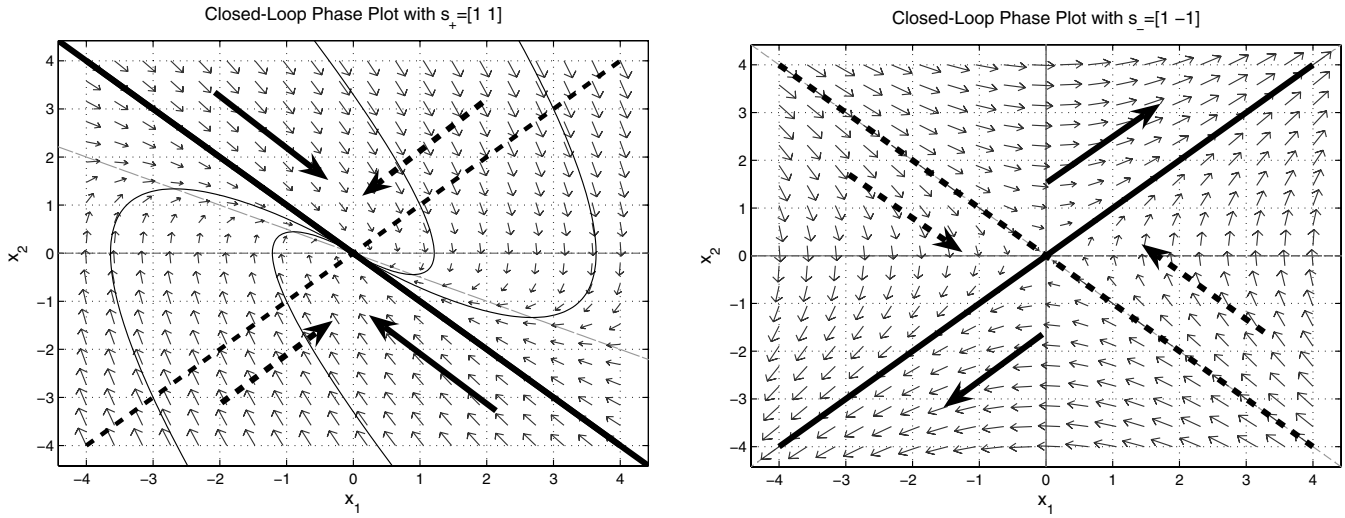

Fig. 2 Phase portraits of the double integrator closed-loop system.

dynamics. The second-order model uses a zero-order model for the actuator dynamics, while the third-order model incorporates a first-order model of the actuator dynamics. We demonstrate the feasibility of our proposed synergetic control design based on either of the wing-rock models. Additionally, sliding mode controllers are developed based on the second- and third-order dynamic models. The sliding surface construction method for sliding mode control can also be used to construct a stable invariant manifold for the synergetic optimal control. Thus, for the synergetic and the sliding mode controller designs, we can use the same manifold for each control design method. We then compare the performance of each controller in the closed-loop configuration. Finally, we explore the problem of control design using a reduced-order model where we use the third-order model as a "truth" model, while a simplified second-order model as a design model. The controllers designed using the design model are tested on the truth third-order model.

A. Control Design Using Second-Order Dynamic Model

The second-order dynamic model [29] of the wing rock using zero-order dynamic actuator model has the form:

$$\ddot{\phi} = \alpha_1\phi + \alpha_2\dot{\phi} + \alpha_3|\phi|\dot{\phi} + \alpha_4|\dot{\phi}|\dot{\phi} + \alpha_5\phi^3 + u \tag{57}$$

where the parameter values of α_i are as follows: $\alpha_1 = -36.1063$, $\alpha_2 = 0.665537$, $\alpha_3 = -2.75214$, $\alpha_4 = 0.00954708$, and $\alpha_5 = 41.6621$. We represent the second-order nonlinear equation (57) in the following state-space format:

$$\begin{bmatrix}\dot{x}_1\\ \dot{x}_2\end{bmatrix} = \begin{bmatrix} x_2 \\ \alpha_1 x_1 + \alpha_5 x_1^3 + \alpha_2 x_2 + \alpha_3|x_1|x_2 + \alpha_4|x_2|x_2\end{bmatrix} + \begin{bmatrix}0\\1\end{bmatrix}u = \boldsymbol{A}(\boldsymbol{x}) + Bu \tag{58}$$

where $x_1 = \phi$ and $x_2 = \dot{\phi}$ are the state variables. We use the procedure of Slotine and Li [32] to construct the manifold, where

$$\sigma(x_1, x_2) = \left(\frac{\mathrm{d}}{\mathrm{d}t} + \lambda\right)x_1 = \dot{x}_1 + \lambda x_1 = x_2 + \lambda x_1 = \underbrace{[\lambda \quad 1]}_{=S}\boldsymbol{x} \tag{59}$$

We select $\lambda = 6$, which is the same value as in Fernand and Downing [29].

1. Sliding Mode Controller Design

As in [15] on p. 228, we design a sliding mode controller that consists of two terms: 1) the equivalent control term u_{eq} and 2) the discontinuous control term u_d. The equivalent control term is determined by solving $\dot{\sigma}(x_1, x_2) = 0$, from which we obtain

$$u_{\mathrm{eq}} = -\left(\alpha_1 x_1 + \alpha_5 x_1^3 + \alpha_2 x_2 + \alpha_3|x_1|x_2 + \alpha_4|x_2|x_2 + \lambda x_2\right) \tag{60}$$

Note that if one applies the equivalent control alone, then the trajectories of the system driven by this equivalent controller will move parallel to the sliding surface $\sigma(x_1, x_2) = 0$. This is because the equivalent control forces $\dot{\sigma}(x_1, x_2) = 0$. The role of the discontinuous control term u_d is to "bend" the trajectories toward the sliding surface and to compensate for any matched uncertainties. We use the following form of u_d:

$$u_d = -K\mathrm{sign}(\sigma(x_1, x_2)) \tag{61}$$

Therefore, the two-term sliding mode control law, consisting of the terms given by Eqs. (60) and (61) takes the form,

$$u = u_{\mathrm{eq}} + u_d = -\left(\alpha_1 x_1 + \alpha_5 x_1^3 + \alpha_2 x_2 + \alpha_3|x_1|x_2 + \alpha_4|x_2|x_2 + \lambda x_2\right) - K\mathrm{sign}(\lambda x_1 + x_2) \tag{62}$$

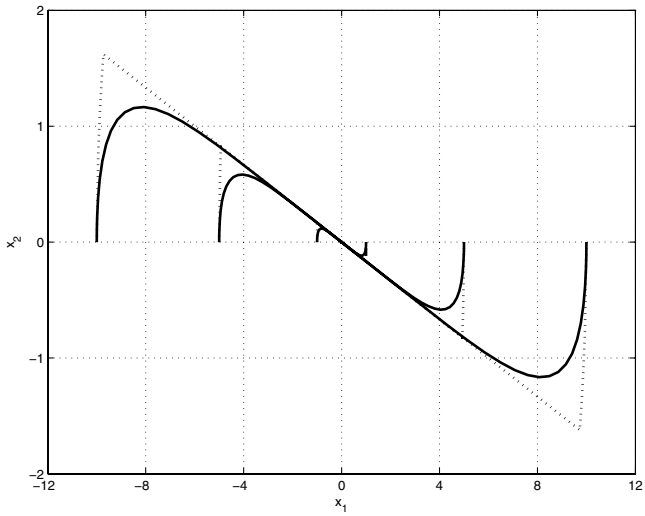

Fig. 3 Trajectories of the closed-loop second-order dynamic model of the wing rock. Solid line trajectories are produced by the synergetic controller. Dotted line trajectories are produced by the sliding mode controller.

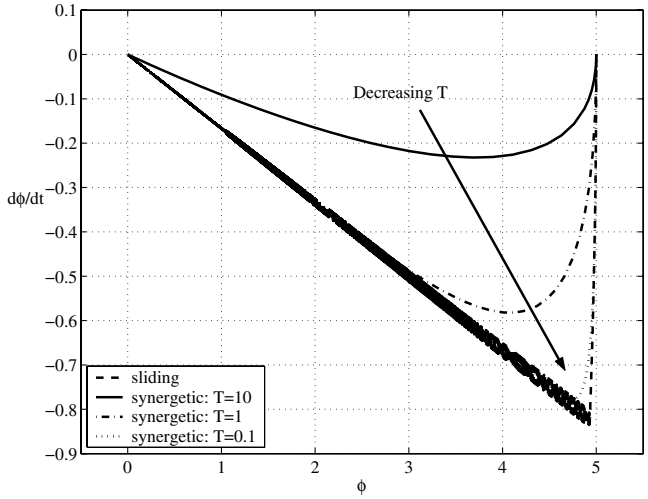

Fig. 4 Closed-loop system: phase-plot dependence on the parameter T.

2. Synergetic Controller Design

We use the same manifold $\sigma = \sigma(x_1, x_2) = 0$ as in the sliding mode controller synthesis. The manifold $\sigma = 0$ in the synergetic controller design leads to the control law that optimizes the functional

$$\int_{t_0}^{\infty} (T^2\dot{\sigma}^2 + \sigma^2)\,\mathrm{d}t = \int_{t_0}^{\infty} (T^2(\lambda\dot{x}_1 + \dot{x}_2)^2 + (\lambda x_1 + x_2)^2)\,\mathrm{d}t \tag{63}$$

with T as a design parameter. As follows from the preceding sections, the control law that minimizes the functional (63) satisfies the first-order differential equation $T\dot{\sigma} + \sigma = 0$. Solving this differential equation, we obtain

$$\begin{aligned} u &= -(TSB)^{-1}(TSA(\boldsymbol{x}) + S\boldsymbol{x}) = u_{\mathrm{eq}} - (TSB)^{-1}\sigma \\ &= -\left(\alpha_1 x_1 + \alpha_5 x_1^3 + \alpha_2 x_2 + \alpha_3 |x_1| x_2 + \alpha_4 |x_2| x_2 + \lambda x_2\right) \\ &\quad - T^{-1}(\lambda x_1 + x_2) \end{aligned} \tag{64}$$

Note that the synergetic controller comprises two terms, where the second term of the synergetic controller is a smooth approximation of the discontinuous term of the sliding mode controller.

3. Numerical Results

Figure 3 shows the closed-loop systems' phase portraits for six different initial conditions. Trajectories of the closed-loop system driven by the synergetic control law are plotted using solid lines, while the trajectories of the closed-loop system driven by the sliding mode control law (62) are plotted using dotted lines. We observe that in the absence of modeling uncertainties, the performance of the synergetic control law is comparable to that of the sliding controller in driving the closed-loop system trajectories to the origin. Both controllers successfully suppress sustained limit-cycle oscillations induced by the wing-rock phenomenon. Closed-loop trajectories generated by both control laws converge to the manifold $\sigma(x_1, x_2) = 0$. However, the synergetic control law smoothly drives trajectories from their initial conditions toward $\sigma(x_1, x_2)$ while the sliding mode control law forces the trajectories to hit the sliding surface in finite time and then move along the sliding surface toward the origin.

The effect of different values of the design parameter T, appearing in the synergetic controller, on the closed-loop trajectories is illustrated in Figs. 4 and 5. In these figures, we show plots of trajectories versus time of the closed-loop dynamic system (58) driven by 1) the variable structure sliding mode control, where the sign function is approximated using a steep tangential-sigmoid function [i.e., $\mathrm{sign}(\boldsymbol{x}) \approx \tanh(1000\boldsymbol{x})$], and 2) synergetic controller implemented using various values of T. We can see in Fig. 4 that as the value of T decreases, trajectories approach the manifold $\sigma(x_1, x_2) = 0$ more rapidly. As expected, when T decreases, trajectories of the closed-loop system driven by the synergetic control law resemble those of the closed-loop system employing the sliding mode controller as shown in the phase portrait of Fig. 4 and the time-response plots in Fig. 5. This is because for smaller values of T, the term $T^{-1}(\lambda x_1 + x_2)$ better approximates $\mathrm{sign}(\lambda x_1 + x_2)$ in the neighborhood of the manifold $\sigma = 0$. Observe the presence of trajectory chattering in the system driven by the sliding mode control. On the other hand, the closed-loop system trajectories driven by the synergetic control are free from chattering. Chattering is clearly seen along the manifold $\mathcal{M}$ in Fig. 4. However, due the magnitude scale used, the trajectory chattering of $\dot{\phi}$ is not clearly visible in the time-history plot of $\dot{\phi}$ in Fig. 5.

B. Control Design Using Third-Order Dynamical Model

The first-order actuator δ_a model combined with a generic second-order wing-rock dynamics model results in the following dynamic model of wing rock [25,28,30,31]:

$$\dddot{\phi} = \alpha_1\phi + \alpha_2\dot{\phi} + \alpha_3\dot{\phi}^3 + \alpha_4\phi^2\dot{\phi} + \alpha_5\phi\dot{\phi}^2 + \beta\delta_a \tag{65}$$

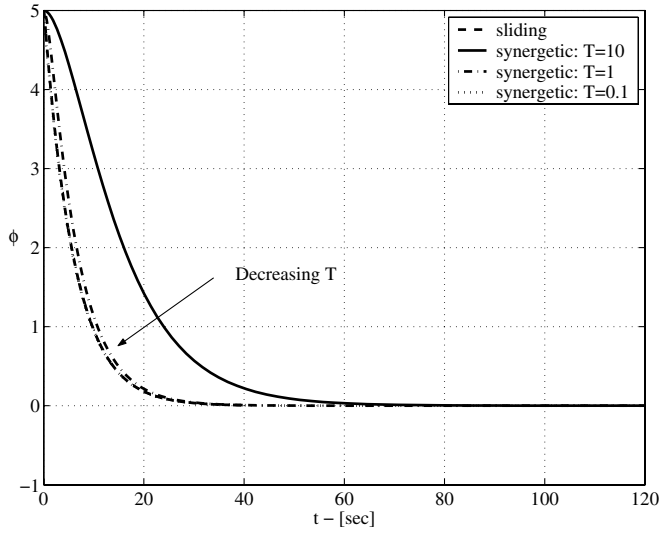

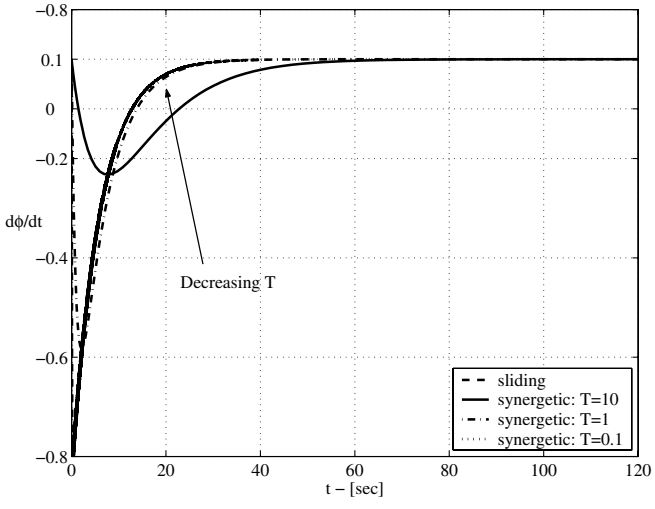

Fig. 5 Closed-loop system: time response performance dependence on the parameter T.

$$\tau\dot{\delta}_a = -\delta_a + u \tag{66}$$

We represent the above model in the following state-space format:

$$\begin{bmatrix}\dot{x}_1\\ \dot{x}_2\\ \dot{x}_3\end{bmatrix} = \begin{bmatrix} x_2 \\ \alpha_1 x_1 + \alpha_2 x_2 + \alpha_3 x_2^3 + \alpha_4 x_1^2 x_2 + \alpha_5 x_1 x_2^2 + \beta x_3 \\ -\frac{1}{\tau}x_3 \end{bmatrix} + \begin{bmatrix}0\\0\\ \frac{1}{\tau}\end{bmatrix} u = \boldsymbol{A}(\boldsymbol{x}) + Bu \tag{67}$$

where $x_1 = \phi$ and $x_2 = \dot{\phi}$. The state $x_3 = \delta_a$ represents the first-order actuator. The values of the model parameters are as follows: $\alpha_1 = -0.0148927$, $\alpha_2 = 0.0415424$, $\alpha_3 = 0.01668756$, $\alpha_4 = -0.06578382$, $\alpha_5 = 0.08578836$, $\beta = 1.5$, and $\tau = 1/15$. These values correspond to an aircraft flight at an angle of attack of 21.5 deg and can be found in [25,28,30,31].

In our construction of the two-dimensional invariant manifold, we again use the method of Slotine and Li [32] to obtain

$$\begin{aligned}\sigma(x_1, x_2, x_3) &= \left(\frac{\mathrm{d}}{\mathrm{d}t} + \lambda\right)^2 x_1 = \dot{x}_2 + 2\lambda x_2 + \lambda^2 x_1 \\ &= \alpha_1 x_1 + \alpha_2 x_2 + \alpha_3 x_2^3 + \alpha_4 x_1^2 x_2 + \alpha_5 x_1 x_2^2 + \beta x_3 \\ &\quad + 2\lambda x_2 + \lambda^2 x_1\end{aligned} \tag{68}$$

where after some numerical experiments we selected $\lambda = 10$ to reduce excessive overshoot. We mention that because $\sigma(x_1, x_2, x_3) = (\frac{\mathrm{d}}{\mathrm{d}t} + \lambda)^2 x_1$, the closed-loop system restricted to the manifold $\sigma(x_1, x_2, x_3) = 0$ will have a double pole at $-\lambda = -10$.

In the following sections, we design sliding mode and synergetic controllers around the above invariant manifold.

1. Sliding Mode Controller Construction

Using the manifold defined by Eq. (68), we first compute the equivalent control u_{eq} for the third-order model by solving the equation $\dot{\sigma}(x_1, x_2, x_3) = 0$, that is,

$$\dot{\sigma}(\boldsymbol{x}) = \nabla_{\boldsymbol{x}}\sigma(\boldsymbol{x})^{\top}\dot{\boldsymbol{x}} = \nabla_{\boldsymbol{x}}\sigma(\boldsymbol{x})^{\top}(\boldsymbol{A}(\boldsymbol{x}) + Bu) = 0$$

where $\nabla_{\boldsymbol{x}}\sigma(\boldsymbol{x})$ is the gradient of $\sigma = \sigma(\boldsymbol{x})$, with respect to $\boldsymbol{x} = [x_1 \quad x_2 \quad x_3]^{\top}$. After some manipulations, we obtain

$$u_{\mathrm{eq}} = -\frac{\tau}{\beta}\left(\alpha_1 x_2 + \alpha_2\dot{x}_2 + 3\alpha_3 x_2\dot{x}_2 + \alpha_5(x_2^3 + 2x_1 x_2\dot{x}_2) - \frac{\beta}{\tau}x_3 + 2\lambda\dot{x}_2 + \lambda^2 x_2\right) \tag{69}$$

Note that the expression for $\dot{x}_2$ is given by the state equation (67). We construct the same type of sliding mode controller as for the second-order wing-rock dynamical model,

$$u = u_{\mathrm{eq}} + u_d$$

where

$$u_d = -K\mathrm{sign}(\sigma(x_1, x_2, x_3)), \qquad K = 10 \tag{70}$$

Hence the sliding controller for the third-order wing-rock dynamical model takes the form,

$$\begin{aligned}u = u_{\mathrm{eq}} + u_d = -\frac{\tau}{\beta}&\left(\alpha_1 x_2 + \alpha_2\dot{x}_2 + 3\alpha_3 x_2\dot{x}_2 \right.\\ &\left. + \alpha_5\left(x_2^3 + 2x_1 x_2\dot{x}_2\right) - \frac{\beta}{\tau}x_3 + 2\lambda\dot{x}_2 + \lambda^2 x_2\right)\\ &- K\mathrm{sign}\left(\dot{x}_2 + 2\lambda x_2 + \lambda^2 x_1\right)\end{aligned} \tag{71}$$

2. Synergetic Controller Construction

The synergetic control law is obtained by solving the first-order differential equation,

$$T\dot{\sigma}(x_1, x_2, x_3) + \sigma(x_1, x_2, x_3) = 0$$

Solving this differential equation for u, we obtain

$$\begin{aligned}u = -\frac{\tau}{\beta}&\left(\alpha_1 x_2 + \alpha_2\dot{x}_2 + 3\alpha_3 x_2\dot{x}_2 + \alpha_5\left(x_2^3 + 2x_1 x_2\dot{x}_2\right)\right.\\ &\left. - \frac{\beta}{\tau}x_3 + 2\lambda\dot{x}_2 + \lambda^2 x_2\right) - \frac{\tau}{\beta}T^{-1}\left(\dot{x}_2 + 2\lambda x_2 + \lambda^2 x_1\right)\end{aligned} \tag{72}$$

where $T = 0.01$. Note again that the expression for $\dot{x}_2$ is provided by the state model (67). We mention again that the second term in Eq. (72) can be interpreted as a smooth approximation to the discontinuous term of the sliding mode controller, that is, the second term in Eq. (71).

3. Numerical Results

As predicted, and expected, both controllers drive closed-loop trajectories toward the origin. Figure 6 consists of two subfigures depicting trajectories, in the (x_1, x_2) plane, of the third-order closed-loop systems driven by the sliding mode and synergetic controllers, respectively.

The value of the design parameter T in the synergetic controller was selected so that the closed-loop system trajectories, driven by this controller, converge to the origin at the same rate as those driven by the sliding mode controller. We conclude from plots in Fig. 6 that to achieve comparable behavior of x_1 to that of the sliding mode controller, the state x_2 of the synergetic controller driven system undergoes large excursions induced by the actuator state x_3. Such overshoots can be reduced by increasing the value of the parameter T. As a consequence of increasing T, trajectory convergence of the synergetic controller toward the origin occurs at a lower rate. Note that increasing T essentially correlates with decreasing the synergetic control law gains. We can see in Fig. 7 that closed-loop state variable trajectories of closed-loop wing-rock dynamics driven by either sliding mode or synergetic controller converge to the origin. However, rapid convergence to the origin in the synergetic controller driven system comes with a price in that x_2 and x_3 initially experience excessively large overshoots that may not be desirable. A large excursion of the actuator state x_3 results in large deviations of the roll rate $\dot{\phi}$, that is, x_2.

When we increase the value of T from $T = 0.01$ to $T = 2.5$, trajectory overshoots of the closed-loop dynamics driven by the synergetic controller decrease. Transient discrepancies between

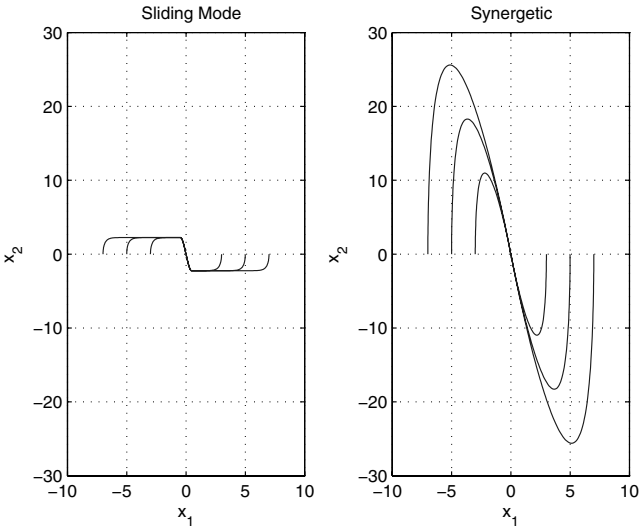

Fig. 6 State variable trajectories of the third-order closed-loop wing-rock dynamic system in the ϕ–$\dot{\phi}$ coordinates.

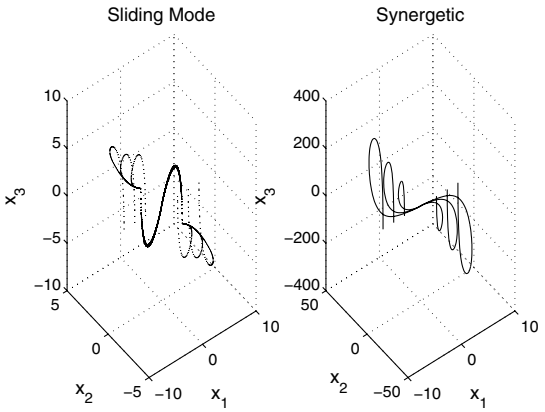

Fig. 7 State trajectories of the third-order closed-loop wing-rock dynamic systems driven by the sliding mode and synergetic controllers, respectively.

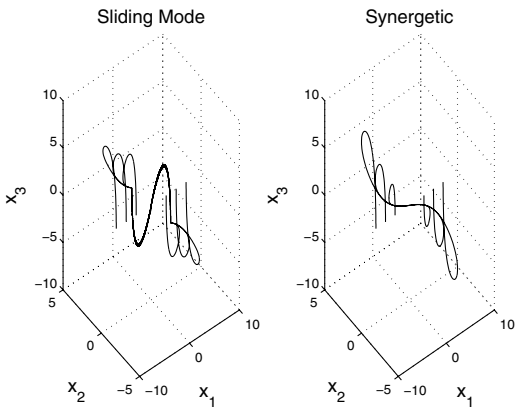

Fig. 9 Three-dimensional state trajectories of the closed-loop systems driven by the sliding mode and low-gain synergetic controllers.

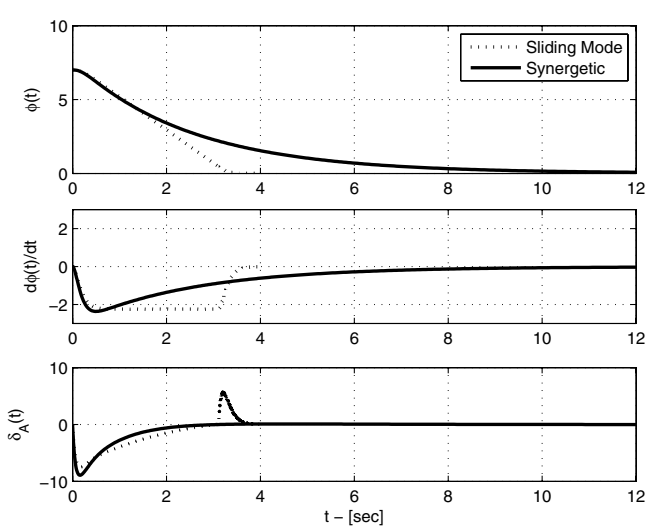

Fig. 8 Time response comparison between sliding mode control driven trajectories (dotted lines) and low-gain synergetic controller driven trajectories (solid lines).

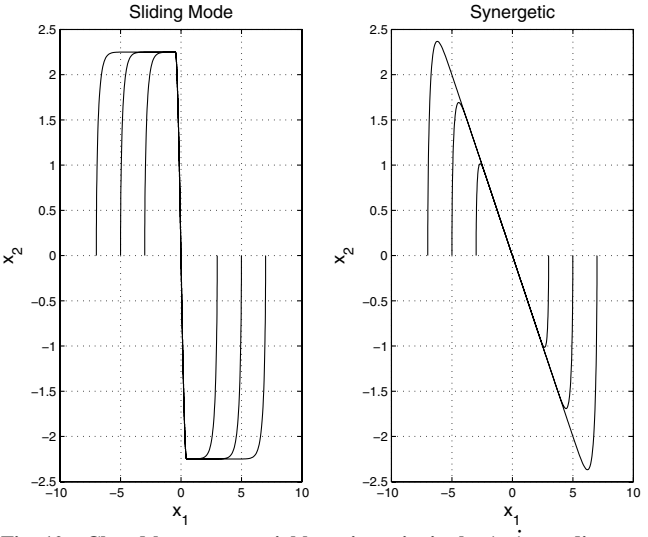

Fig. 10 Closed-loop state variable trajectories in the ϕ–$\dot{\phi}$ coordinates: performance comparison of sliding mode and low-gain synergetic controller driven third-order closed-loop systems.

trajectories of the closed-loop dynamics driven by the sliding mode and synergetic control laws become smaller. In Fig. 8, we show plots of time histories of the state variables of the closed-loop systems driven by the sliding mode and synergetic controller, respectively. State variables of the closed-loop system driven by the sliding mode controller are denoted by dotted lines while those driven by the synergetic controller are denoted by solid lines. The synergetic controller with larger values of T does not induce excessive overshoots. State variables driven by the synergetic controller approach the origin more smoothly. In particular, the state variable x_3 driven by the sliding mode controller undergoes an abrupt jump at approximately $t = 3$ s, while x_3 driven by the synergetic controller smoothly approaches zero. Peaks of transient dynamics of the closed-loop state variables x_2 and x_3 driven by both controllers are quite similar. However, these plots also indicate that state variables of the closed-loop system driven by the low-gain synergetic controller reach their steady-state values at a slower rate. The sliding mode controller driven closed-loop state variables reach steady state at approximately 4 s, while those driven by the synergetic controller reach steady state at approximately 9 s.

As stated before, increasing the parameter T implies reducing the synergetic controller gain. Gain reduction implies that less effort is demanded from the actuator. Using $T = 2.5$ compared to $T = 0.01$ for the synergetic control law design reduces the maximum overshoot of the actuator state variable. Low gain design relaxes the demand for actuation. Hence, a direct consequence of low actuator state excursion is the reduced roll rate dynamics. In Figs. 9 and 10, we show overshoot reduction of the state variables x_2 and x_3 when $T = 2.5$. In Fig. 9, the scales of the x_3 axis are the same, so the maximum x_3 overshoot of the closed-loop dynamics driven by the sliding mode and synergetic controllers are approximately the same. Figure 10 shows that the peak values of x_2 of the closed-loop dynamics driven by both the sliding mode and the synergetic controllers are similar. We conclude that excessive overshoots in the closed-loop dynamics driven by the synergetic controller decrease as lower gain, that is, a larger T is applied to the synergetic controller.

C. Control Design Using Reduced-Order Model

To accurately model the truth behavior of a dynamic system it may require a high-order model. Such a model may be too complex for use in control synthesis. A simplified model, referred to as a "design model," is usually developed for controller design. Even if the truth model is used for control design, it may lead to a complicated control law. Comprehensive treatments of controller and observer design for systems with neglected high-order dynamics can be found, for example, in [33] on pp. 252–268 and in [34] on pp. 333–350.

In the two preceding cases, we used the truth model as the design model, so the performance of the sliding mode and synergetic controllers were assessed on dynamical models that were also used for the purpose of control design. The second-order wing-rock dynamical model (58) is driven by the control laws (62) and (64) which were developed based upon Eq. (58). Similarly, the third-

order wing-rock dynamical model (67) is driven by the control laws (71) and (72) where both controllers were developed using Eq. (67).

Here, we investigate the case of designing synergetic and sliding mode control laws for wing-rock suppression using a lower-order model. Then, these controllers are employed to control a higher-order representation of the dynamics. To serve our purpose, the third-order wing-rock model represents the truth model. We obtain our design model from the third-order model by neglecting the actuator dynamics. Thus, the design model has the form,

$$\dot{\boldsymbol{x}}_r = \begin{bmatrix} \dot{x}_1 \\ \dot{x}_2 \end{bmatrix} = \begin{bmatrix} x_2 \\ \alpha_1 x_1 + \alpha_2 x_2 + \alpha_3 x_2^3 + \alpha_4 x_1^2 x_2 + \alpha_5 x_1 x_2^2 \end{bmatrix} + \begin{bmatrix} 0 \\ \beta \end{bmatrix} u \tag{73}$$

$$= \begin{bmatrix} 0 & 1 \\ \alpha_1 + \alpha_5 x_2^2 & \alpha_2 + \alpha_3 x_2^2 + \alpha_4 x_1^2 \end{bmatrix} \begin{bmatrix} x_1 \\ x_2 \end{bmatrix} + \begin{bmatrix} 0 \\ \beta \end{bmatrix} u = A_r \boldsymbol{x}_r + B_r u \tag{74}$$

where the subscript r denotes "reduced." The parameters α_i in Eq. (73) have been given previously and are the same as those in Eq. (67).

1. Controller Construction Using the Design Model

We now proceed with the design procedure using the second-order design model derived above. The invariant manifold is constructed similarly to Eq. (59):

$$\sigma(\boldsymbol{x}) = S_r \boldsymbol{x}_r = [\,\lambda \quad 1\,]\boldsymbol{x}_r \tag{75}$$

Using the matrices A_r and B_r defined in Eq. (74) along with S_r from Eq. (75), we obtain the synergetic controller

$$u_{r\,\text{synergetic}} = -(TS_rB_r)^{-1}(TS_rA_r + S_r)\boldsymbol{x}_r = -(TS_rB_r)^{-1}TS_rA_r - (TS_rB_r)^{-1}S_r\boldsymbol{x}_r \tag{76}$$

The sliding mode controller has the form,

$$u_{r\,\text{sliding mode}} = -(TS_rB_r)^{-1}TS_rA_r\boldsymbol{x}_r - K\text{sign}(S_r\boldsymbol{x}_r) \tag{77}$$

As in the preceding design cases, the synergetic and sliding mode controller structures are related. Both controllers use the equivalent control component. However, the sliding mode controller uses a discontinuous component, while the synergetic control employs a smooth approximation to the discontinuous component of the sliding mode controller.

We now connect the control laws (76) and (77) to drive the third-order model (67), so that the closed-loop third-order system becomes

$$\begin{bmatrix} \dot{x}_1 \\ \dot{x}_2 \\ \dot{x}_3 \end{bmatrix} = \begin{bmatrix} x_2 \\ \alpha_1 x_1 + \alpha_2 x_2 + \alpha_3 x_2^3 + \alpha_4 x_1^2 x_2 + \alpha_5 x_1 x_2^2 + \beta x_3 \\ -\frac{1}{\tau} x_3 \end{bmatrix} + \begin{bmatrix} 0 \\ 0 \\ \frac{1}{\tau} \end{bmatrix} u_r \tag{78}$$

where u_r can be either $u_{r\,\text{synergetic}}$ or $u_{r\,\text{sliding mode}}$. There are two design parameters, T and λ, whose influence on the closed-loop dynamics (78) will be investigated next.

2. Numerical Results

Adjustable parameters λ and T must be carefully selected because high values of either λ or T lead to unstable solutions, while very low values of either λ or T induce oscillations with frequency inversely proportional to the value of either λ or T. In Fig. 11, we show a family of stable closed-loop solutions for various values of λ. Our experiments indicate that for a fixed value of T, where $T \leq 0.1$, a stabilizing controller requires the value of λ to be less than 3. Thus, all λs such that $0 < \lambda \leq 3$ are feasible values for fixed $T \leq 0.1$. However, as can be seen in Fig. 11, lower values of λ induce higher frequency oscillations around the manifold $\mathcal{M}$. Hence, slower motion along the manifold $\mathcal{M}$ will reduce oscillations around $\mathcal{M}$.

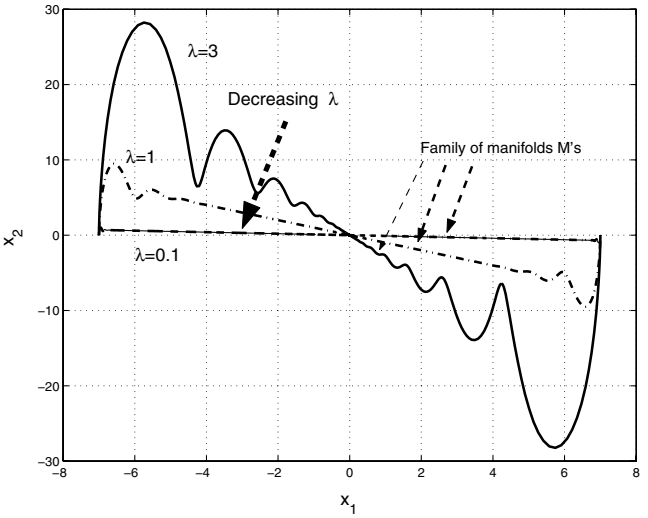

Fig. 11 The effect of λ. Higher values of λ correspond to rapid movement toward the origin. However, higher values of λ induce oscillatory dynamics around the manifold $\mathcal{M}$.

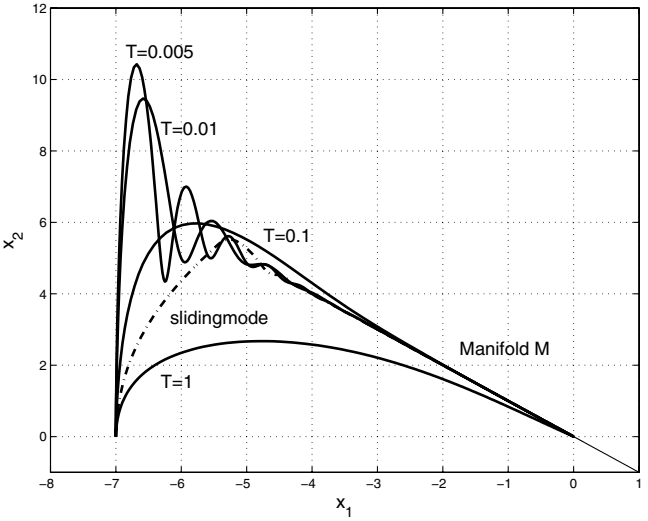

Fig. 12 The effect of T on the performance of the synergetic controller. A lower value of T corresponds to rapid movement toward the manifold $\mathcal{M}$. However, a lower value of T induces oscillation around the manifold $\mathcal{M}$.

The parameter T also affects stability and performance of the closed-loop wing-rock suppression. As T gets higher, the gain of the second term of Eq. (76) becomes smaller. Such low-gain control action prevents excessive oscillations. In Fig. 12, we show a family of stable solutions with various values of Ts using $\lambda = 1$. We can see that smaller values of T induce oscillations around the manifold $\mathcal{M}$ with higher frequency. Although lower values of T, yielding higher gains for the second term of Eq. (76), lead to rapid motion toward the manifold $\mathcal{M}$, their effect on higher frequency oscillations around $\mathcal{M}$ may not be desirable. As a comparison, the closed-loop solution driven by the sliding mode is also shown in Fig. 12 as the plot with the dash-dotted line. We conclude that the selection of $T = 0.1$ may lead to the synergetic design with comparable performance to that of the sliding mode design.

Plots of state variables versus time are presented in Figs. 13 and 14, where we used $\boldsymbol{S}_r = [\,1 \quad 1\,]$, the sliding mode control gain $K = 10$,

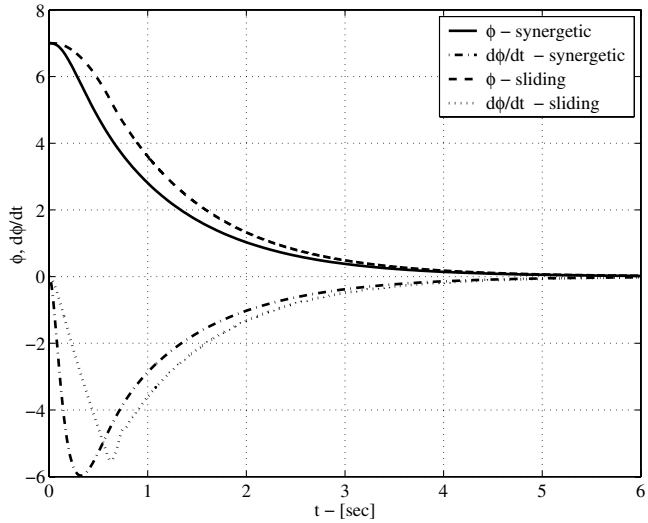

Fig. 13 Comparison of $\phi(t)$ and $\dot{\phi}(t)$ trajectories driven by synergetic and sliding mode controllers.

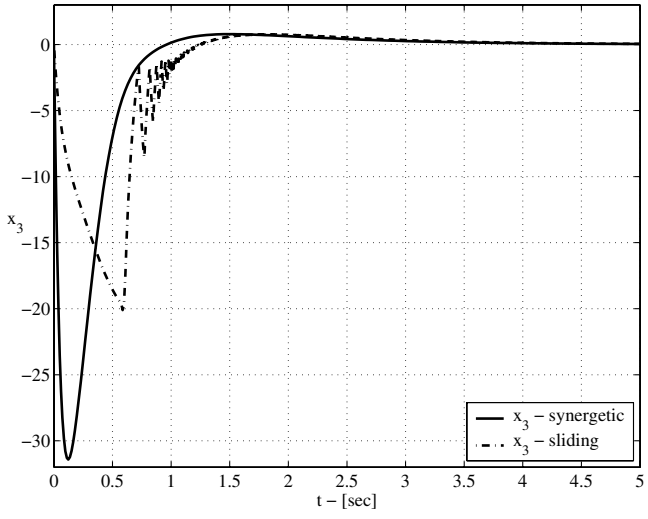

Fig. 14 Comparison of x_3 trajectories driven by synergetic and sliding mode controllers.

and the synergetic control design parameter $T = 0.1$. These values were selected so that the states ϕ and $\dot{\phi}$ driven by both synergetic and sliding mode controllers would have approximately similar time responses. From Eq. (78), we see that the controller u_r directly affects the state variable x_3. We show in Fig. 14 time responses of x_3 driven by both synergetic and sliding mode controllers. When x_3 is driven by the sliding mode control, it experiences chattering. However, we see that x_3 is smooth when it is driven by the synergetic control. The transient peak of x_3 when it is driven by the synergetic control, as it is also seen in the phase portraits in Figs. 11 and 12, is larger than the peak of x_3 driven by the sliding mode control.

X. Concluding Remarks

A variety of sliding mode controllers has been proposed and applied to a large number of engineering problems [35–37] including nonlinear problems [38,39]. The behavior of nonlinear dynamic systems driven by the synergetic control to some extent resembles that of nonlinear dynamic systems driven by sliding mode control. Hence, one can benefit by analyzing synergetic controllers from the point of view of sliding mode control combined with an optimal control. Explorations in sliding mode control may, indeed, be beneficial to the synergetic control. Such explorations may reveal further optimality characteristics. The synergetic control approach offers a closed-form analytical solution to a class of nonlinear optimal control problems. The proposed control design methodology is attractive because it only requires the associated first-order differential equation. Indeed, as the problem of optimal control design is further restricted to linear time-invariant dynamical systems, optimal control solution generated by the synergetic control is the same as the solution generated by the LQR with the special form of the performance criterion. In summary, the paper contributions are as follows:

1) Synergetic control approach was shown to follow from both the necessary (Euler–Lagrange) and the sufficiency (HJB) conditions for optimality, resulting in the first-order differential equation to develop a synergetic controller.

2) Connections between the synergetic control approach and the variable structure sliding mode control method were established.

3) Synergetic control was shown to provide the same controller as the LQR with a special performance index for the case of linear time-invariant dynamic systems.

4) Synergetic control was used to successfully design a nonlinear controller for wing-rock stabilization using existing nonlinear dynamic models.

5) Synergetic controllers were shown to be effective in the nonlinear wing-rock stabilization application. This included reducing overshoot in the actuator state variable and by providing a smoother transition of state variables to the stable condition.

References

[1] Owens, D., *Multivariable and Optimal Systems*, Academic Press, London, U.K., 1981.

[2] Lee, E., and Markus, L., *Foundations of Optimal Control Theory*, The SIAM Series in Applied Mathematics, Wiley, New York, 1968.

[3] Pinch, E., *Optimal Control and Calculus of Variations*, Oxford Science Publications, Oxford University Press Inc., New York, 1993.

[4] Bryson, A., and Ho, Y.-C., *Applied Optimal Control*, Hemisphere, New York, 1975.

[5] Athans, M., and Falb, P., *Optimal Control: An Introduction to the Theory and Its Applications*, Lincoln Laboratory Publications, McGraw–Hill, New York, 1966.

[6] Bellman, R., and Kalaba, R., *Dynamic Programming and Modern Control Theory*, Academic Press, New York, 1965.

[7] Kolesnikov, A. A. (ed.), *Modern Applied Control Theory: Synergetic Approach in Control Theory*, TRTU, Moscow-Taganrog, 2000.

[8] Kolesnikov, A., "Synergetic Control of the Unstable Two-Mass System," *Fifteenth International Symposium on Mathematical Theory of Networks and Systems*, Univ. of Notre Dame Press, South Bend, IN, Aug. 2002.

[9] Kolesnikov, A., "Synergetic Control for Electromechanical Systems," *Fifteenth International Symposium on Mathematical Theory of Networks and Systems*, Univ. of Notre Dame Press, South Bend, IN, Aug. 2002.

[10] Kondratiev, I., Dougal, R., Santi, E., and Veselov, G., "Synergetic Control for m-Parallel Connected DC-DC Buck Converters," *35th Annual IEEE Power Electronics Specialists Conference*, IEEE, Piscataway, NJ, 2004, pp. 182–188.

[11] Santi, E., Monti, A., Li, D., Proddutur, K., and Dougal, R., "Synergetic Control for Power Electronics Applications: A Comparison with the Sliding Mode Approach," *Journal of Circuits, Systems, and Computers*, Vol. 13, No. 4, 2004, pp. 737–760.

[12] Jiang, Z., and Dougal, R., "Synergetic Control of Power Converters for Pulse Current Charging of Advanced Batteries from a Fuel Cell Power Source," *IEEE Transactions on Power Electronics*, Vol. 19, No. 4, July 2004, pp. 1140–1150.

[13] Terekhov, V., Tyukin, I., and Prokhorov, D., "Adaptive Control on Manifolds with RBF Neural Networks," *Proceedings of the 39th IEEE Conference on Decision and Control*, IEEE, Piscataway, NJ, Dec. 2000, pp. 3831–3836.

[14] Nusawardhana, and Żak, S., "Optimality of Synergetic Controllers," *Proceedings of the 2006 ASME International Mechanical Engineering Congress and Exposition*, American Society of Mechanical Engineers, Chicago, IL, 5–10 Nov. 2006.

[15] DeCarlo, R., Żak, S. H., and Matthews, G., "Variable Structure Control of Nonlinear Multivariable Systems: A Tutorial," *Proceedings of the IEEE*, Vol. 76, No. 3, March 1988, pp. 212–232.

[16] Khalil, H., *Nonlinear Systems*, 2nd ed., Prentice–Hall, Upper Saddle River, NJ, 1996.

[17] Edwards, C., and Spurgeon, S., *Sliding Mode Control: Theory and Applications*, Taylor and Francis, London, 1998.
[18] Utkin, V., and Young, K., "Methods for Constructing Discontinuity Planes in Multidimensional Variable Structure Systems," *Automation and Remote Control (English Translation)*, Vol. 39, No. 10, 1978, pp. 1466–1470.
[19] Utkin, V., *Sliding Modes in Control and Optimization*, Springer–Verlag, Berlin, 1992.
[20] Żak, S. H., *Systems and Control*, Oxford Univ. Press, New York, 2003.
[21] Gelfand, I., and Fomin, S., *Calculus of Variations*, Prentice–Hall, Englewood Cliffs, NJ, 1963.
[22] Leitmann, G., *The Calculus of Variation and Optimal Control*, Mathematical Concepts and Methods in Science and Engineering, Plenum Press, New York, 1981.
[23] Anderson, B., and Moore, J., *Optimal Control: Linear Quadratic Methods*, Prentice–Hall, Englewood Cliffs, NJ, 1989.
[24] Bertsekas, D., *Dynamic Programming and Optimal Control*, Vols. 1–2, Athena Scientific, Belmont, MA, 1995.
[25] Elzebda, J., Nayfeh, A., and Mook, D., "Development of an Analytical Model of Wing Rock for Slender Delta Wings," *Journal of Aircraft*, Vol. 26, No. 8, 1989, pp. 737–743.
[26] Guglieri, G., and Quagliotti, F., "Analytical and Experimental Analysis of Wing Rock," *Nonlinear Dynamics*, Vol. 24, No. 2, 2001, pp. 129–146, Kluwer Academic Publishers.
[27] Hsu, C.-H., and Lan, C., "Theory of Wing Rock ," *Journal of Aircraft*, Vol. 22, No. 10, 1985, pp. 920–924.
[28] Konstadinopoulos, P., Mook, D., and Nayfeh, A., "Subsonic Wing Rock of Slender Delta Wings," *Journal of Aircraft*, Vol. 22, No. 3, 1985, pp. 223–228.
[29] Fernand, J., and Downing, D., "Discrete Sliding Mode Control of Wing Rock," *AIAA Guidance, Navigation and Control Conference*, AIAA, Washington, D.C., 1–3 Aug. 1994, pp. 46–54; also AIAA Paper 1994-3543.
[30] Gazi, V., and Passino, K., "Direct Adaptive Control Using Dynamic Structure Fuzzy Systems," *Proceedings of the American Control Conference*, IEEE, Piscataway, NJ, June 2000, pp. 1954–1958.
[31] Passino, K., *Biomimicry for Optimization, Control, and Automation*, Springer–Verlag, London, 2005.
[32] Slotine, J., and Li, W., *Applied Nonlinear Control*, Prentice–Hall, Englewood Cliffs, NJ, 1991.
[33] Corless, M., Leitmann, G., and Ryan, E., *Control of Uncertain Systems with Neglected Dynamics*, edited by A. S. I. Zinober, Chap. 12, Deterministic Control of Uncertain Systems, Peter Peregrinus Ltd., Michael Faraday House, Six Hills Way, Stevenage, Herts. SG1 2AY, U.K., 1990, pp. 252–268.
[34] Żak, S., and Walcott, B., *State Observation of Nonlinear Control Systems via the Method of Lyapunov*, edited by A. S. I. Zinober, Chap. 16, Deterministic Control of Uncertain Systems, Peter Peregrinus Ltd., Michael Faraday House, Six Hills Way, Stevenage, Herts. SG1 2AY, U.K., 1990, pp. 333–350.
[35] Hess, R., and Wells, S., "Sliding Mode Control Applied to Reconfigurable Flight Control Design," *Journal of Guidance, Control, and Dynamics*, Vol. 26, No. 3, May–June 2003, pp. 452–462.
[36] Shima, T., Idan, M., and Golan, O., "Sliding-Mode Control for Integrated Missile Autopilot Guidance," *Journal of Guidance, Control, and Dynamics*, Vol. 29, No. 2, March–April 2006, pp. 250–260.
[37] Utkin, V., Guldner, J., and Shi, J., *Sliding Mode Control in Electro-Mechanical Systems*, Taylor and Francis, Philadelphia, PA, 1999.
[38] Chin, C. L. W., "Adaptive Decoupled Fuzzy Sliding-Mode Control of a Nonlinear Aeroelastic System," *Journal of Guidance, Control, and Dynamics*, Vol. 29, No. 1, Jan.–Feb. 2006, pp. 206–209.
[39] Zhou, D., Mu, C., and Xu, W., "Adaptive Sliding-Mode Guidance of a Homing Missile," *Journal of Guidance, Control, and Dynamics*, Vol. 22, No. 4, July–Aug. 1999, pp. 589–594.